Impacts of Hurricane Ian along the Low-Lying Southwest Florida Coast (USA) in 2022: Lessons Learned

Ping Wang*, Elizabeth L. Royer, Kendal Jackson, and Sophia Gutierrez

School of Geosciences University of South Florida Tampa, Florida 33620, U.S.A.







Wang, P.; Royer, E.L.; Jackson, K., and Gutierrez, S., 0000. Impacts of Hurricane Ian along the low-lying southwest Florida coast (USA) in 2022: Lessons learned. *Journal of Coastal Research*, 00(00), 000–000. Charlotte (North Carolina), ISSN 0749-0208.

Hurricane Ian made landfall in the low-lying, densely populated, and developed southwestern Florida coast on 28 September 2022 as a large and slow-moving category 4 hurricane. Various U.S. federal and state agencies collected a large and comprehensive data set, including pre- and poststorm airborne LIDAR topography, in situ water level and wave measurements at numerous locations before, during, and after the storm, and poststorm high-water marks over a large area. This study reports results from a series of poststorm field investigations including ground observations of beach-dune erosion and deposition, catastrophic damage to various infrastructure, and widespread distribution of non-biodegradable materials washed into the estuary and numerous mangrove islands. Hurricane Ian induced large-scale inundation in lowlying southwest Florida, submerging all the barrier islands bordering Charlotte Harbor estuary, all the islands within the estuary, and up to 5 km into the mainland. Dense tree-type vegetation limited the landward penetration of beach-dune erosion and overwash deposition along the barrier islands. Net sand-volume loss from the beach-dune system ranged 10-25 m³/m and was controlled by the deep submergence of the system during the peak of the storm. The extremely high storm surge of up to 5.2 m above mean sea level generated by Hurricane Ian caused severe damage to the built environments over a large area. High storm waves superimposed on the elevated water level, reaching 1.2 m at the seaward edge of vegetated dunes, contributed to the destruction along the barrier islands. Hurricane Ian distributed a tremendous amount of non-biodegradable artificial debris over a large area and into sensitive natural environments, including numerous mangrove islands, barrier-island interior wetlands, and the estuary waterbody. Measures to prevent materials such as single-use plastics, insulation fibers, and household appliances from being washed into sensitive environments should be a significant part of prestorm preparation.

ADDITIONAL INDEX WORDS: Storm surge, flooding, beach erosion, dune erosion, storm damage, storm preparation, Florida.

INTRODUCTION

Hurricanes, generally known as tropical cyclones, constitute major natural hazards that have caused, and will continue to cause, significant economic damage as well as human deaths (Emanuel, 2003). The influence of climate change on the frequency and intensity of hurricanes and resultant impacts to coastal areas have been the topics of numerous studies (Emanuel, Sundararajan, and William, 2008; IPCC, 2022, 2023; Knutson et al., 2010). Although the overall trend of hurricane frequency and intensity is not as clear as, for example, global temperature increase and sea-level rise, the trend of rapidly increasing monetary damage to developed coastal areas is clear (AghaKouchak et al., 2020; Mendelsohn et al., 2012; Peduzzi et al., 2012; Pielke et al., 2008). The increasing monetary costs of storm impacts are largely controlled by the rapid human development of the coastal areas, particularly coastal cities, despite the increasingly well-established and well-communicated climate-related hazards and their future trends (Dawson et al., 2018; Gencer et al., 2018). Therefore, accurate assessment (Simpson et al., 2021) and effective mitigation/adaptation (Grafakos et al., 2018; McPhearson *et al.*, 2018) are essential to coping with and minimizing damages induced by hurricanes. The catastrophic impact of Hurricane Ian in southwest Florida provides an opportunity to examine the successes and failures of society as a whole in responding to this extremely energetic storm and in coastal management in general (Beck and Wang, 2019).

Hurricane Ian made landfall in southwestern Florida on 28 September 2022 as a large and slow-moving category 4 hurricane (Bucci et al., 2023). Hurricane Ian caused over 150 direct and indirect human deaths and over \$112 billion (USD) in damage (as of April 2023), making it the costliest hurricane in Florida's history and the third costliest in U.S. history behind Hurricane Katrina in 2005 and Hurricane Sandy in 2012 (Bucci et al., 2023). The track of Hurricane Ian is shown in Figure 1. At 0200 UTC 28 September, the eye of the 110 knots (kt) (204 km/h) hurricane passed directly over the Dry Tortugas (Florida, U.S.A.). Hurricane Ian intensified later and reached its peak intensity of 140 kt (259 km/h, a category 5 hurricane) at 1200 UTC 28 September. Hurricane Ian weakened slightly during the next several hours before it made landfall on the mostly pristine barrier island of Cayo Costa at 1905 UTC 28 September with an intensity of 130 kt (241 km/h). An hour and a half later, at 2035 UTC, the center of Hurricane Ian's large eye made another landfall near Punta Gorda, on the very densely populated, low-lying north shore of Charlotte Harbor estuary, with an estimated intensity of 125 kt (232 km/h) (Bucci et al., 2023).

DOI: 10.2112/JCOASTRES-D-24-00003.1 received 7 January 2024; accepted in revision 22 March 2024; corrected proofs received 12 April 2024; published pre-print online 23 April 2024.

^{*}Corresponding author: pwang@usf.edu

[©]Coastal Education and Research Foundation, Inc. 2024



Figure 1. Best track positions, center pressure, and maximum wind speed for Hurricane Ian, 27–29 September 2022 (modified from Clark, Murshid, and Weeks, 2023).

Overall, Hurricane Ian made four landfalls over low-lying areas at a slow forward-moving speed without rapid loss of strength (Figure 1). The first landfall was at the southwest coast of Cuba on 27 September 2022 as a strong category 3 hurricane with maximum sustained wind speed of 110 kt (204 km/h) (Bucci et al., 2023). The second and third landfalls were only 1.5 hours apart along the southwest Florida coast on 28 September 2022, at Cayo Costa and Punta Gorda, respectively. The Cayo Costa landfall came with a maximum sustained wind speed of 130 kt (241 km/h), or a strong category 4 hurricane. The storm only weakened slightly to 125 kt (232 km/h) at the Punta Gorda landfall. The fourth landfall was at Georgetown, South Carolina, on 1 October 2022 as a 70 kt (130 km/h) category 1 hurricane. The most energetic landfalls in terms of wind velocity, size of the storm, and storm forward movement speed occurred in southwest Florida (Figure 1), which was the focus area of this study. The extremely energetic atmospheric forcing over a shallow, broad, and gentle continental shelf generated very high storm surge flooding over expansive low-lying terrain and caused catastrophic damage over a large area.

A large amount of data was collected by various U.S. agencies, e.g., National Oceanic and Atmospheric Administration (NOAA), U.S. Geological Survey (USGS), and Florida Department of Environmental Protection (FDEP), before, during, and after the passage of Hurricane Ian. Pre- and poststorm airborne LIDAR surveys were conducted to capture detailed morphological changes. Detailed aerial views of storm impacts were captured by aerial photography and videography. The elevated

water level and its temporal and spatial patterns caused by the storm were measured by numerous water-level sensors installed by USGS a day or two before the storm landfall, in addition to long-term NOAA tide gauges. Overland wave height at several locations was also measured by the USGS gauges. In addition to sensor measurements, elevations of high-water marks were mapped by several trained teams shortly after the storm. In this study, these data sets were analyzed, and *in situ* field observations were conducted along developed and pristine sections of the coast, including sandy beaches and dunes, various infrastructure such as roads and vessel-supporting structures, various types of buildings, and mangrove islands.

As part of FDEP's poststorm assessment, Clark, Murshid, and Weeks (2023) provided systematic county-by-county documentation of Hurricane Ian's impact along the southwest Florida coast. This study focused on the various factors controlling the storm damage to both the natural and built environment. The resilience of this low-lying coast (including both natural and heavily developed areas) against an extremely energetic storm event was examined.

Despite its overall low elevation and high vulnerability to flooding due to sea-level rise and storm surge, the population in southwest coastal Florida has grown rapidly in recent decades (Palm and Bolsen, 2023). Furthermore, an earlier landfall in this area by the strong category 4 Hurricane Charley in 2004, although smaller and faster moving, did not have significant impact on recent population growth. Hurricane Ian directly impacted over 1.5 million people in southwest

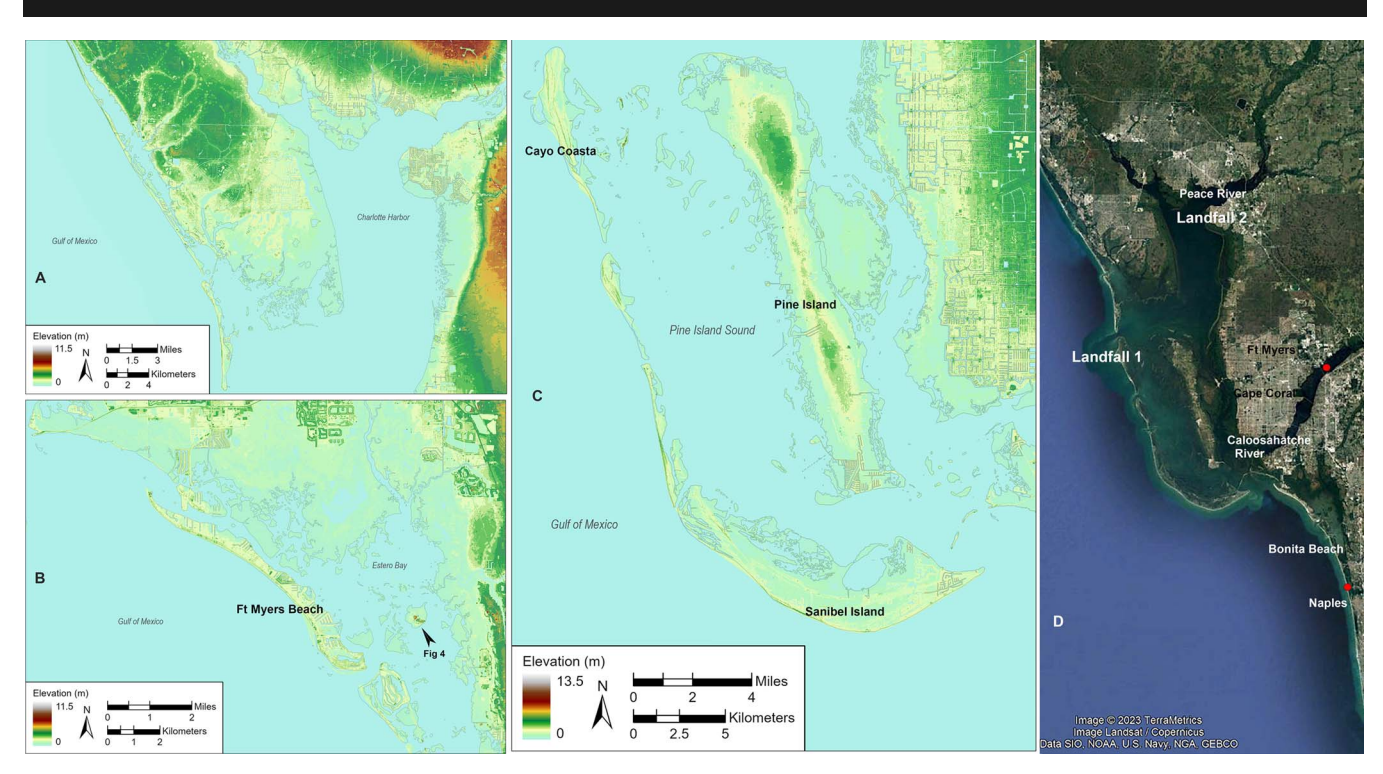


Figure 2. Charlotte Harbor estuary and the surrounding low-lying areas: (A) northern Charlotte Harbor; (B) southern Charlotte Harbor, showing the densely developed Estero Island (aka, Ft. Myers Beach) bordering Estero Bay; (C) middle Charlotte Harbor, showing the pristine Cayo Costa island at the north end and Sanibel Island at the south, and the large Pine Island in the middle; and (D) aerial view of the entire Charlotte Harbor, showing dense development at places. The general location of the estuary is shown in Figure 1. The red markers are long-term NOAA tide stations.

Florida. The overall goal of this paper is to summarize the lessons learned from this catastrophic hurricane in terms of resiliency in a low-lying and densely populated coastal areas, and implications for future resilience building.

This paper is organized as follows. After the "Introduction," the study area (including the barrier islands, the estuary and its numerous islands, and the rivers) is briefly described. The rapidly increasing and dense development in this flooding-prone area is briefly reviewed. This is followed by a description of methodology used in this study. In the "Results" section, the hurricane impacts in various developed and pristine environments are described. The "Discussion" section summarizes the lessons learned on coastal resiliency against extreme storms.

Study Area

From the perspective of general coastal settings, the strong category 4 Hurricane Ian made landfall in an estuarine environment, *i.e.* Charlotte Harbor (Figure 2). The Charlotte Harbor estuary is composed of a chain of barrier islands along the southeast Gulf of Mexico coast. The barrier islands are of different lengths, widths, and orientations (Davis, 1994; Wang and Beck, 2022), and they exhibit variable degrees of human development, ranging from nearly pristine, *e.g.*, Cayo Costa State Park at the Florida landfall 1 site (Figure 2C, D), to almost completely developed, *e.g.*, Estero Island, where Ft. Myers Beach (Figure 2B, D) is located.

As made apparent in the digital elevation model (DEM) based on a recent airborne LIDAR survey (Figure 2), the elevations of the terrestrial landforms encompassing Charlotte Harbor and the numerous islands within the estuary are very low, mostly below 3 m relative to mean sea level (MSL). The extensive low-elevation areas include both pristine and heavily developed zones. It is worth noting that buildings, bridges, and other modern aboveground infrastructure were omitted from the DEM shown in Figure 2.

Employing the same airborne LiDAR-based DEM, Figure 3 shows that if the sea level is raised by 3 m above MSL, then a large portion of the coastal area around Charlotte Harbor will be submerged. The submerged area would include all the barrier islands separating Charlotte Harbor from the Gulf of Mexico. There are no sand dunes on the barrier islands, pristine or heavily developed, that exceed the elevation of +3 m MSL. The humid climate, generally low wind speed, and high content of large shell debris in the sediment hinder the development of high dunes. The often highly developed mainland coast landward of Charlotte Harbor (Figure 3B) would be submerged up to 5 km inland. As illustrated in the following text, Hurricane Ian's storm surge exceeded 3 m over a large area.

The numerous islands within Charlotte Harbor would be submerged by the 3 m elevated water level (Figure 3). The several small areas that extend above 3 m elevation are predominately associated with Indigenous shell mounds. One of the larger Native American archaeological sites in this area is located on northern Pine Island (Figure 3B). The highest elevation within the study area, up to 10 m above MSL, excluding modern

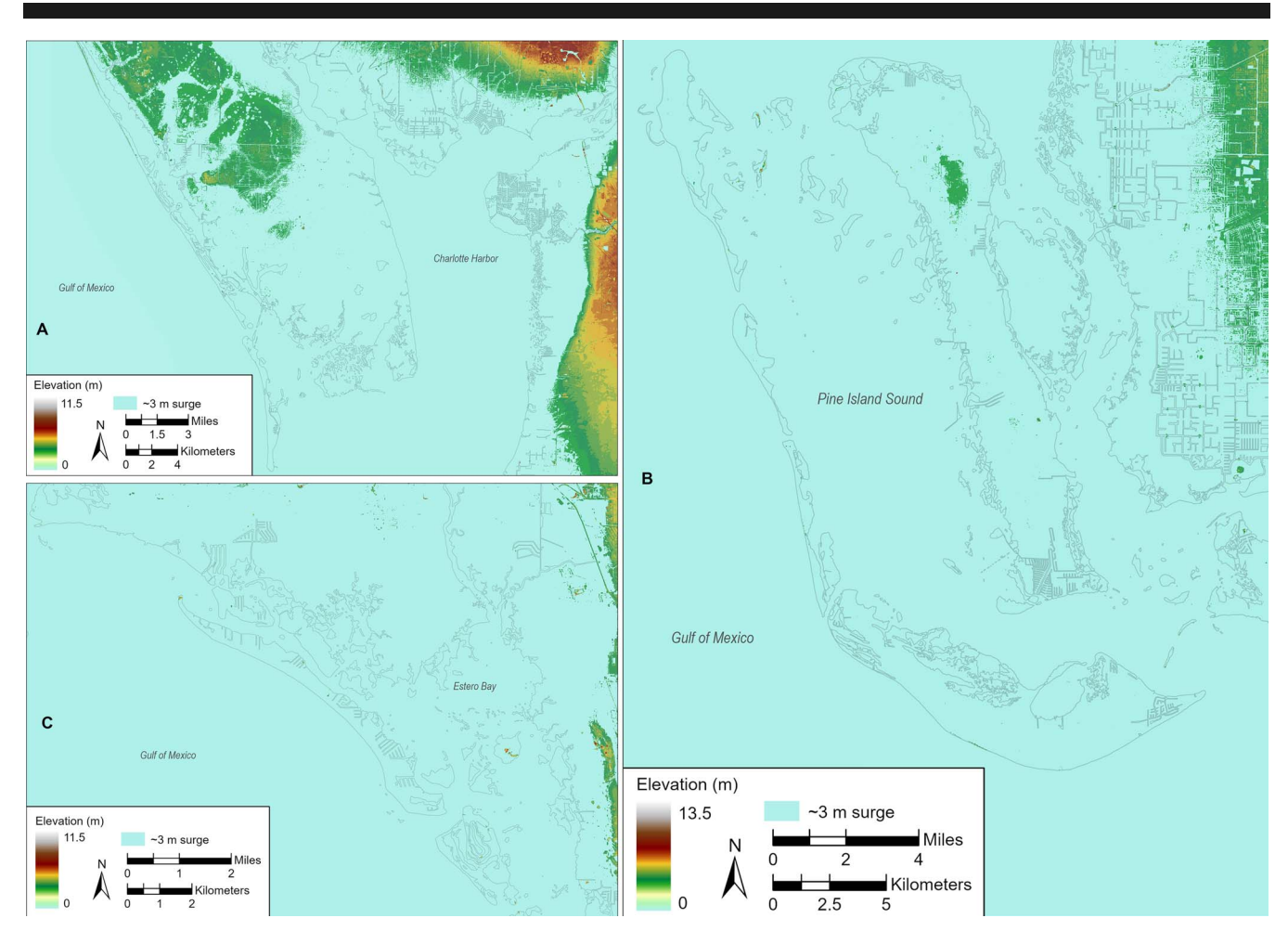


Figure 3. Charlotte Harbor and the surrounding areas under an elevated sea level of 3 m: (A) northern Charlotte Harbor; (B) southern Charlotte Harbor with the densely developed Estero Island submerged; and (C) middle Charlotte Harbor with densely developed Pine Island and mainland coast submerged.

buildings, is measured at the Mound Key Archaeological State Park (Figure 4) in Estero Bay (Figure 3C)—an anthropogenic island constructed by Indigenous peoples (Thompson *et al.*, 2020). A considerable portion of the mound complex is raised well above 3 m relative to MSL (Figure 4C), affording the opportunity to observe storm effects below, at, and above the maximum surge elevation at this archaeological site. Field observations at Mound Key indicate that the surficial cultural shell deposits below the maximum surge elevation were washed quite clean of fine and organic sediments, illustrating a bright white color (Figure 4D, E). This contrasts starkly with the typical brownish-gray color of coastal shell mound deposits due to the abundance of decayed plant debris, *i.e.* humic matter (Figure 4F). Figure 4D depicts a prominent scarp and wrack line that extend along the maximum surge elevation at Mound Key.

Three major rivers enter Charlotte Harbor estuary, the Peace River at the NE, the Myakka River at the NW, and the Caloosahatchee River at the SW ends of the estuary (Figure 2D). The Peace River mouth area, where Florida landfall 2 site is located (Figure 2D), is heavily developed. The Caloosahatchee River mouth area, located to the south of Florida landfall 1 site

(Figure 2D) and impacted by tremendous onshore forcing with the highest measured storm surge, is also heavily developed, including the fast-growing cities of Cape Coral and Ft. Myers. Both areas would be submerged by the 3 m elevated water level. Hurricane Ian's storm surge exceeded 3 m MSL in both areas. In addition, the storm surge also traveled up the rivers and compounded with large discharges from the heavy rainfall, which caused flooding substantially up the river. Inland flooding is beyond the scope of this paper.

Another major factor contributing to the catastrophic impact of Hurricane Ian is the large, dense, and rapidly increasing population in this low-lying area. Before the impact of Hurricane Ian in September 2022, Palm and Bolsen (2023) identified that housing demand and house prices in southwest Florida, including the area of Hurricane Ian's impact, were rising faster than anywhere else in the United States, despite the very low overall elevation and apparent risks associated with sea-level rise and storm impacts. Their study examined the perspectives of southwest Florida homeowners and real-estate agents on flood risks, as well as their subsequent decision making. Palm and Bolsen (2023) surveyed 461 homeowners living in southwest Florida in

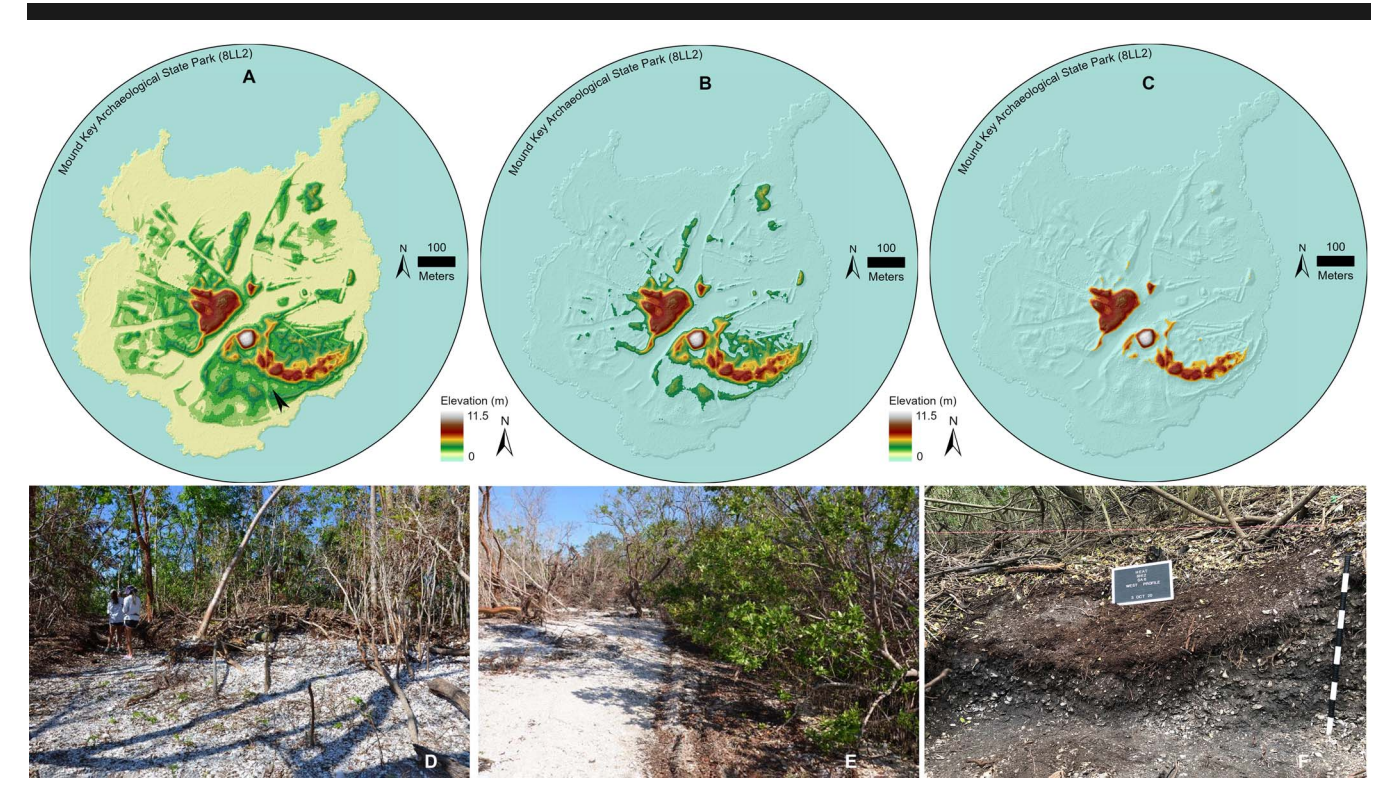


Figure 4. DEM of Mound Key Archaeological State Park in Estero Bay (location is shown in Figure 2B). (A) DEM relative to MSL, where black arrow indicates the location of the photos shown in the lower panels. (B) DEM with 1.5 m elevated sea level. (C) DEM with 3 m elevated sea level; note that a portion of the mount is still above water level. (D) Wrack line and scarp induced by Hurricane Ian. (E) Shell washed clean by the elevated water; compare with panel F. (F) Shell with plant debris.

2018 and 198 southwest Florida real-estate agents in 2020. They found that prospective homebuyers continued to seek coastal property and largely disregarded apparent flood risks, even when the potential hazards were illustrated to them with aerial photos depicting potential submergence. Furthermore, in the survey by Palm and Bolsen (2023), real-estate agents reported that lenders and appraisers seemed not to discount property even when it was highly susceptible to coastal flooding.

This rather troublesome perception by both homeowners and real-estate agents, in southwest Florida and elsewhere, is likely a main driver for population growth in coastal areas in the United States and worldwide, even in low-lying and flood-prone areas. In a study on the housing market in Miami-Dade, Florida, McAlpine and Porter (2018) found that flooding risks have a negative influence on housing prices, although not significant overall. Kim (2020) found that green infrastructure adaptation projects and structure elevation have a positive influence on housing prices in major coastal cities like New York and Miami. However, both studies concluded that the relatively small price change does not seem to have significant influence on population growth driven by housing demand, as documented by Palm and Bolsen (2023).

METHODS

A large variety of data was collected by various agencies before, during, and after the passage of Hurricane Ian. Figure 5

summarizes the extensive data collected by the USGS and NOAA. The study area has two long-term NOAA Tides and Currents Stations (Figure 2D, red markers), which provide temporal trends and statistical parameters. Numerous highwater mark measurements were conducted after the storm over a large area, as controlled by the expansive low elevation (Figure 5). USGS successfully installed a significant number of rapid deployment gauges (pressure sensors) measuring elevated water levels and overland waves during the passage of the storm. These data are valuable in improving current understanding and modeling capability of the evolution of the storm, *i.e.* the strengthening and dissipation of the storm surge and waves.

Aerial photos and videos were collected by NOAA and FDEP immediately after the storm subsided. Airborne LIDAR surveys focusing on the barrier-island beaches were conducted shortly before and immediately after the storm. Detailed morphological changes, particularly those over the subaerial portion of the barrier islands, were captured by the LIDAR data. Clark, Murshid, and Weeks (2023) performed systematic county-by-county poststorm ground investigation.

For this study, series of field observations and measurements were conducted after the storm. Several beach profiles were surveyed using a real-time kinematic GPS. These beach profiles compared well with the LIDAR surveys, which had much more complete spatial coverage. LIDAR data with 1 m horizontal resolution were used here for morphology analysis. Sediment

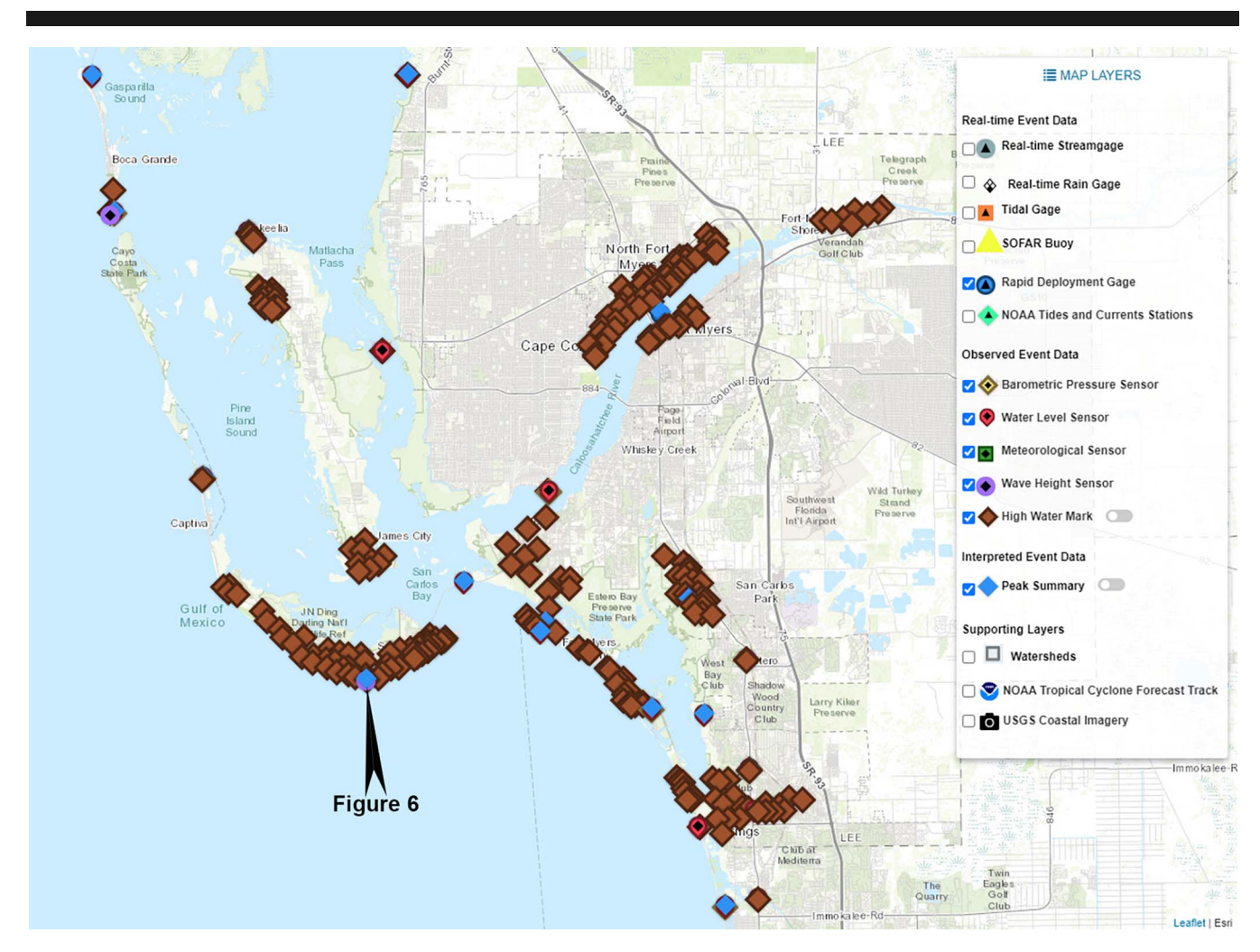


Figure 5. Spatial coverage of USGS and NOAA water level, wave, meteorological parameters, and high-water-mark measurements in the study area. From: https://stn.wim.usgs.gov/FEV/#2022Ian.

cores were collected at various beach-dune-overwash transects and at several mangrove islands. This paper focuses on the morphological changes and various types of damage caused by the storm surge and waves, while sedimentological characteristics of storm overwash are not discussed. Numerous poststorm ground photos were taken in heavily developed areas and in nearby pristine areas. Lessons learned from these photos are discussed in the following text.

RESULTS

The storm surge induced by Hurricane Ian was well documented by the NOAA and USGS gauges, in addition to the poststorm water-mark measurements (Figure 5). Wave forcing superimposed on the elevated water level, also measured by several USGS gauges, likely contributed significantly to the structural damage along the open Gulf of Mexico coast. In this section, Hurricane Ian's storm surge, subsequent damages by wave and surge, and morphological changes are described.

Elevated Water Level Induced by Hurricane Ian

Storm surge and subsequent coastal flooding have been the topic of numerous studies, particularly from the numerical modeling perspective (Brecht *et al.*, 2012; Irish, Resio, and Divoky, 2011; Lin *et al.*, 2012; Mulia *et al.*, 2023; Resio and Westerink, 2008; Woodruff, Irish, and Camargo, 2013). Taking advantage of the rich data set on Hurricane Ian's storm surge, Heidarzadeh *et al.* (2023) simulated both the elevated and depressed water levels as driven by the onshore and offshore forcing, respectively. Here, the focus was on measured storm surge values in terms of their statistical significance and spatial distribution.

First of all, it is worth emphasizing that wave forcing, superimposed on the elevated water level due to storm surge, can play a significant role in impacting both human and natural environments, particularly near the open coast (Cheng, Cossu, and Wang, 2021; Janssen, Lemke, and Miller, 2019; Lemke and Miller, 2020; Miller and Livermont, 2008; Sallenger, 2000). For natural environments, waves are the driving force

for beach-dune erosion and storm overwash (Claudino-Sales, Wang, and Horwitz, 2008, 2010; Wang et al., 2020; Wang and Horwitz, 2007; Wang et al., 2006;). For the developed environments, structural damage caused by Hurricane Ian's wave forcing was apparent, as discussed in the following text. Little is known about wave conditions over land during hurricanes. One of the USGS rapid deployment pressure sensors successfully measured detailed temporal variations in the water level and wave conditions during the passage of Hurricane Ian (Figure 6). This sensor is located just to the south of the landfall 1 site (Figure 5) and likely yielded nearly maximum water level and wave height.

The storm surge reached 13.1 ft (3.99 m) relative to the North American Vertical Datum of 1988 (NAVD88), or 4.12 m above MSL, while unfiltered instantaneous water level reached 16.6 ft (5.06 m) NAVD88, or 5.19 m above MSL (Figure 6A). As discussed earlier (Figures 2 and 3), the elevations of the barrier islands separating Charlotte Harbor and the Gulf of Mexico, the numerous islands with in the estuary, and the extensive coastal zone landward of the estuary are lower than 3 m NAVD88. Thus, the 4 m surge submerged an extensive land area.

The significant wave height measured by the above sensor near the edge of a vegetated dune field reached 4 ft (1.22 m) (Figure 6B). This wave height is much higher than the average wave height in this area, which is lower than 0.3 m (Brutsche and Pollock, 2017; Brutsche et al., 2014). Beach-dune erosion and damage to the overwalk and vegetation were apparent (Figure 6C, D). This wave height also contributed significantly to damaging beachfront structures, as discussed in the following text.

Due to the expansive low elevation in the impacted area, a large and often heavily developed area was submerged significantly by the storm surge. Based on 252 measurements of high-water marks over a large area (Figure 5), a contour map of water depth over land was created and is shown in Figure 7. Overall, 264 km² of area had overland water depth of more than 10 ft (3.05 m). As a comparison, the area of Manhattan Island is roughly 60 km², with a small portion submerged by Hurricane Sandy. In other words, Hurricane Ian submerged about 4.4 Manhattan Islands under more than 3 m water depth. About 718 km² area, or about 12 Manhattan Islands, had water depth of greater than 8 ft (2.44 m) above land. About 1540 km² area, or about 26 Manhattan Islands, had water depth of over 6 ft (1.83 m) aboveground. The deep overland water had direct and/or indirect impacts on critical healthcare, particularly for older adults during and after the passage of Hurricane Ian due to the severe access limitations it created (Bushong and Welch, 2023). Karimiziarani and Moradkhani (2023) tracked Twitter (now X) posts during the passage of Hurricane Ian. Discussions and posts of submergence due to storm surge dominated social media during the passage of the storm.

Sweet et al. (2022) updated the broadly applied NOAA report on projections of sea-level rise and extreme water level probabilities along U.S. coastlines. This most recent NOAA update emphasized projections based on long-term (e.g., more than 50 years) measurements at existing tide stations. There are two long-term NOAA tide stations in the study area: 8725520 Ft. Myers Station (Figure 2D, north red marker) and 8725110 Naples Station (Figure 2D, south red marker). Both stations

have collected water-level measurements since 1965. Extreme water levels were estimated by NOAA at these two stations based on the nearly 70 year measurement history (Figure 8) and are compared with the high-water mark measured by this study. At Barefoot Beach in Bonita Springs, nearly the highest water levels were measured by this study and by USGS. The measured 3.8 m NAVD88 water level (Figure 8A) is roughly 2.5 m higher than the 100 year surge level estimated at the Naples NOAA tide station, which is about 15 km to the south (Figure 8B). At downtown Ft. Myers, which is roughly 20 km landward of the Caloosahatchee River mouth, the measured 2.6 m NAVD88 surge level (Figure 8C) is 1.0 m higher than the 100 year surge level estimated at the NOAA tide station at this location (Figure 8D). It is worth noting that it is possible that the actual storm water level was higher than the elevation indicated by the wrack line. Based on Figure 8, the return period of the Hurricane Ian surge level should be much longer than 100 years.

Damage of Hurricane Ian to the Built Environments

As expected, the extremely fast winds and high overland waves (Figure 6C) superimposed on a tremendously elevated water level (Figure 7) caused catastrophic damage to the built environment. The Charlotte Harbor area, which was directly impacted by Hurricane Ian, is characteristic of a shallow estuary surrounded by expansive low-lying land along both seaward (barrier islands) and landward (mainland) coasts. The estuary is covered with extensive seagrass beds and has numerous islands, with the largest one being the 25-km-long and 1-3-kmwide Pine Island in the middle of southern Charlotte Harbor, which is also referred to as Pine Island Sound (Figure 2C,D). Similar to the Gulf of Mexico and mainland coasts, Pine Island is relatively densely developed. Overall, Charlotte Harbor provides extensive waterfront areas for human development along the Gulf of Mexico and mainland coasts, as well as around the barrier islands and numerous islands within the estuary. Despite the low elevation and apparent high risk of flooding, dense waterfront development occurred during the last few decades (Palm and Bolsen, 2023). The dense waterfront buildings were severely damaged by Hurricane Ian. Because many of the developed areas are surrounded by water within a short distance, tremendous amounts of non-biodegradable and apparently harmful materials were washed into the estuary, as discussed in the following text.

Mobile homes are quite common in southwest Florida and can be easily identified from Google Earth, inland as well as along the waterfront. Figure 9 illustrates an example of a waterfront mobile home community along the landward side of a barrier island. All of the 38 buildings along with the typical waterfront facilities such as boat docks (Figure 9A) were completely destroyed (Figure 9C), with all units being detached from their foundation and washed into the back-barrier estuary environment, an artificially dredged channel in this case (Figure 9D). A large amount of the non-biodegradable and environmentally harmful materials was also washed into the mangrove islands on the other side of the dredged channel (Figure 10C). Mobile homes are simply not built and anchored adequately to sustain hurricane-strength wind or surge. Most of the inland mobile homes were seriously damaged by the strong wind, even when they were higher than the surge level.

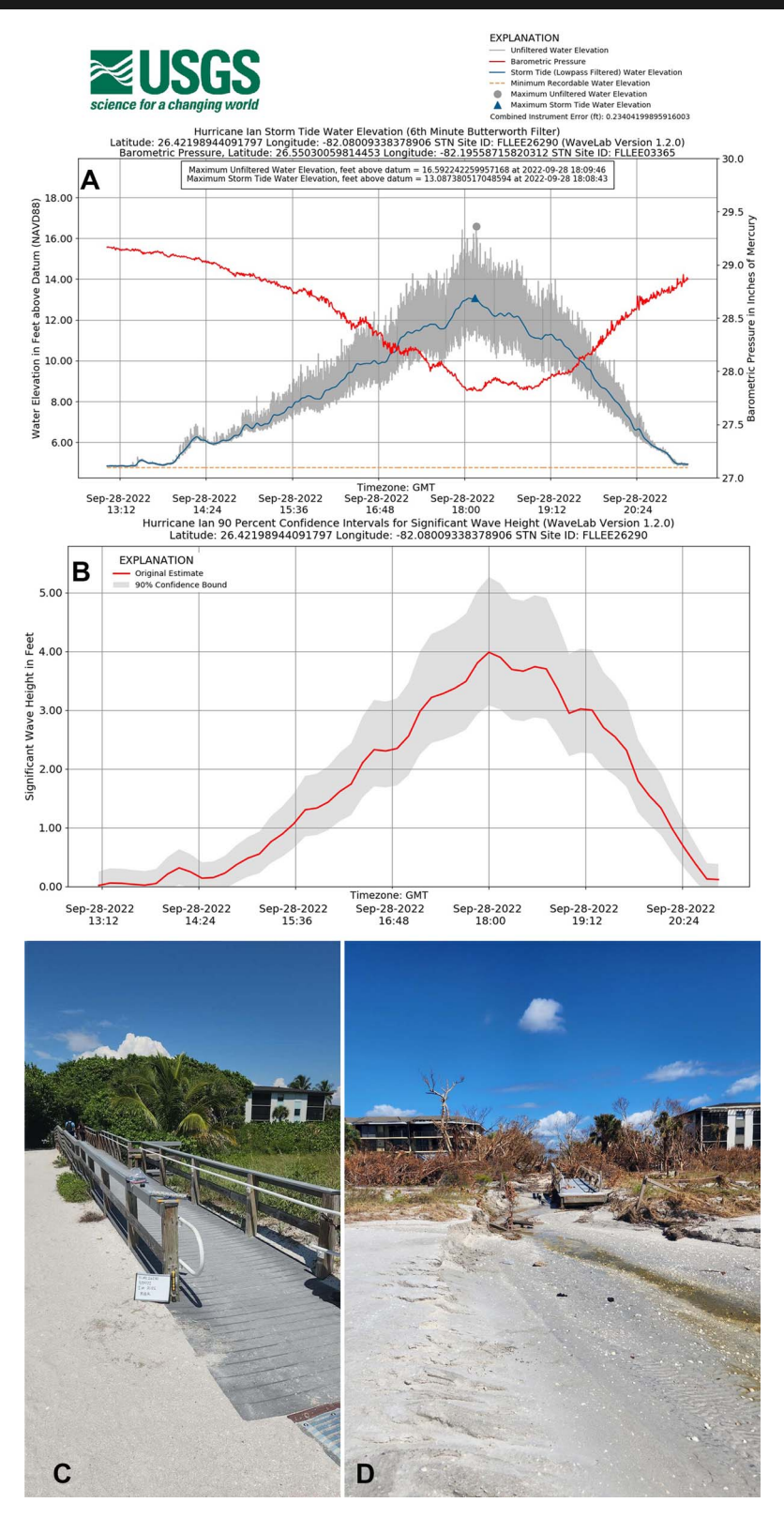


Figure 6. Elevated water level and overland wave conditions measured by a USGS rapid deployment pressure sensor during the passage of Hurricane Ian. The location of the sensor on Sanibel Island is shown in Figure 5. (A) Measured water level (blue line) relative to NAVD88 in feet (1 ft = 0.3048 m). MSL equals 0.125 m below NAVD88 zero. The red line illustrates the measured atmospheric pressure. (B) Measured significant wave height. (C) Ground view of the sensor before the storm. (D) Ground view of the sensor after the storm. From: https://stn.wim.usgs.gov/FEV/#2022Ian.

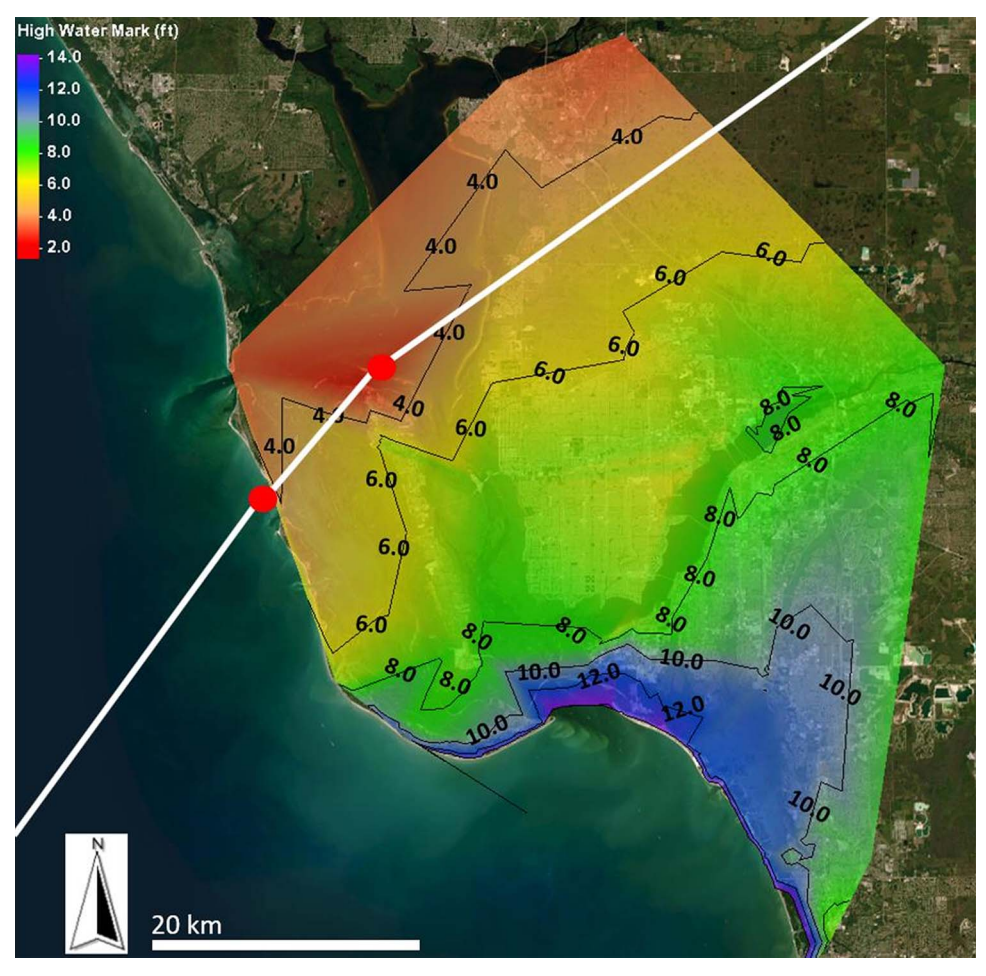


Figure 7. Depth of water overland as contoured based on the measured high-water marks (data points are shown in Figure 5). Data were retrieved from https://stn.wim.usgs.gov/FEV/#2022Ian. Units are in feet, where 1 ft = 0.3048 m.

Systematic county-by-county assessments of infrastructure damage by FDEP are summarized in Clark, Murshid, and Weeks (2023).

Tremendous amounts of artificial debris were washed into the estuary waterbody, with a significant portion trapped in the numerous mangrove islands (Figure 10). Figure 9 provides an example illustrating that everything associated with a waterfront mobile home community was washed into the estuary, ranging from building and insulation materials to all kinds of household goods (Figure 10D) to cars and small vessels (Figure 10C). Many permanent buildings, residential as well as commercial, were also completely destroyed or severely damaged, with the debris washed into the estuary. Permanent waterfront buildings, particularly those along the bayside, carry a similar development scheme to that shown in Figure 9A, although spaced much further apart with slightly higher boat docks and larger vessels. Nevertheless, substantial destruction occurred, with newer and higher buildings faring modestly better than older and lower ones, as expected. The debris washed into the estuary varied widely in size, ranging from an entire house (Figure 10A) to various-sized recreational vessels

(Figure 11A, B) to small pieces of single-use plastic and various household materials (Figure 10C). The debris trapped in the mangrove habitat extended up to 150 m from its shoreline, as estimated based on the NOAA post-Hurricane Ian aerial photos (Figure 11A), now available on Google Earth Pro. It is worth noting that the high-altitude aerial photos taken by NOAA can only resolve large debris within the mangrove islands. The small pieces, mostly plastics, which are visible in many of the ground photos (Figures 9, 10, and 11), cannot be identified in the NOAA aerial photos (Figure 11A). It is, therefore, reasonable to believe that the actual penetration of the non-biodegradable debris, e.g., plastics and insulation fibers (Figure 8A), into the mangrove habitat extended much farther than 150 m. The debris washed into the mangrove islands, particularly the small and numerous plastics and fibrous insulation materials, is almost impossible to remove. Mechanical removal methods using heavy equipment, as shown in Figure 10D, can only remove large debris, while manual removal is not possible due to the vessel-only access, the sheer volume of debris, and its immense spatial distribution.

Along some of the developed barrier islands, large amounts of debris were washed into the interior wetlands from the

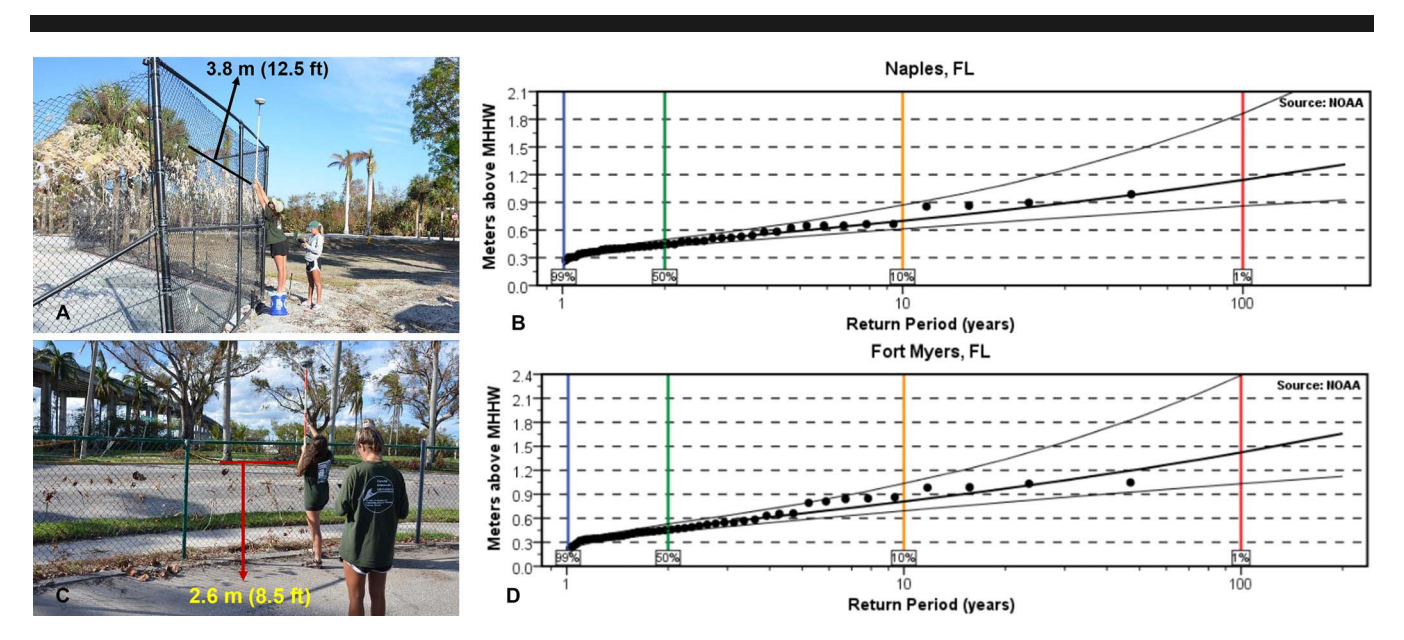


Figure 8. Elevated water level generated by Hurricane Ian, as illustrated by the wrack line on fences, in comparison with estimated extreme water levels by NOAA at the two long-term stations in this area. (A) Wrack line at 3.8 m NAVD88 at Barefoot Beach in Bonita Springs. (B) Extreme water level estimated by NOAA at Naples tidal station, referenced to mean higher high water (MHHW), which is at 0.184 m NAVD88 at this location (https://tidesandcurrents.noaa.gov/est/curves.shtml?stnid=8725110). (C) Wrack line at downtown Ft. Myers at 2.6 m NAVD88. (D) Extreme water level estimated by NOAA at Ft. Myers tidal station, referenced to MHHW, which is at 0.083 m NAVD88 at this location (https://tidesandcurrents.noaa.gov/est/curves.shtml?stnid=8725520).

oceanfront buildings (Figure 12). Compared to the debris washed into the mangrove islands within the estuary as discussed above, this debris is relatively easier to remove, although the process is still time-consuming. Mechanical and manual debris-removal efforts were observed at various locations during field investigations over the winter months after the hurricane impact in September. Long-term ecological impacts of this non-biodegradable debris on the environment, including many pristine mangrove islands, are not clear and are beyond the scope of this study.

Numerous vessels of various sizes were washed on land (Figure 11B) and into mangrove islands (Figure 11A, C). Field investigations revealed that many of these vessels were tied to floating marina types (Figure 11B, top-left inset). A major convenience of floating marinas is that the docks and vessels move together with the rising and falling of tides, making it easier to get on and off the vessels from the dock. Many of the floating docks failed during Hurricane Ian because the extreme storm surge exceeded the height of the anchor pilings. The docks along with the vessels, some quite large (Figure 11B), floated over the anchor pilings onto land (Figure 11B) or into mangrove islands (Figure 11A). Figure 11C illustrates a floating dock and an associated fuel station being washed into a mangrove island. Figure 11B illustrates a foam-filled concrete floating dock washed on land with one piece on the sidewalk of a main road in downtown Ft. Myers (Figure 11B, middle inset). Some of the rather large vessels were still tied to the dock (Figure 11B). A marina directly next to the one shown in Figure 11B with fixed docks fared significantly better, with most of the vessels in place, although some

sunk. These observations suggest that floating docks, although potentially more convenient, can fail catastrophically if storm surge exceeds the height of the anchor pilings. Similar floating dock failures, *i.e.* the docks and vessels floated over the anchor pilings, were observed after Hurricane Idalia (2023) near its landfall site along the Big Bend coast of Florida about 350 km north of Charlotte Harbor.

Beachfront buildings suffered severe damage due to the high waves superimposed on extremely elevated water level. Figure 13 provides several representative examples illustrating the damage to beachfront buildings. Systematic assessment of infrastructure damage can be found in Clark, Murshid, and Weeks (2023). Figure 13A illustrates a newer elevated singlefamily home. The overall structure appears to be in intact, with part of the concrete slab foundation scoured underneath. The second living floor appears to be intact but with visible damage such as at the hot tub. The fibrous insulation material was exposed and trapped behind the damaged fence. This material can be observed at numerous locations, including on many previously pristine mangrove islands (Figures 8A, 9D, 10C, D, and 12). Part of the roof was damaged. It is not clear if the elevated living floor was flooded. The nonliving first floor was severely damaged. Based on the many dangling cables, the first floor likely housed many appliances that were washed away. Many of such appliances, e.g., air-conditioning units, various types of storage tanks, and water heaters, were washed into the backbay and trapped in mangrove islands far from their sources (Figures 9D and 10B, C, D). Although severely damaged, this newer building fared better than the house to the left, which was lifted off the pilings and cannot be seen in this photo. Figure 13B

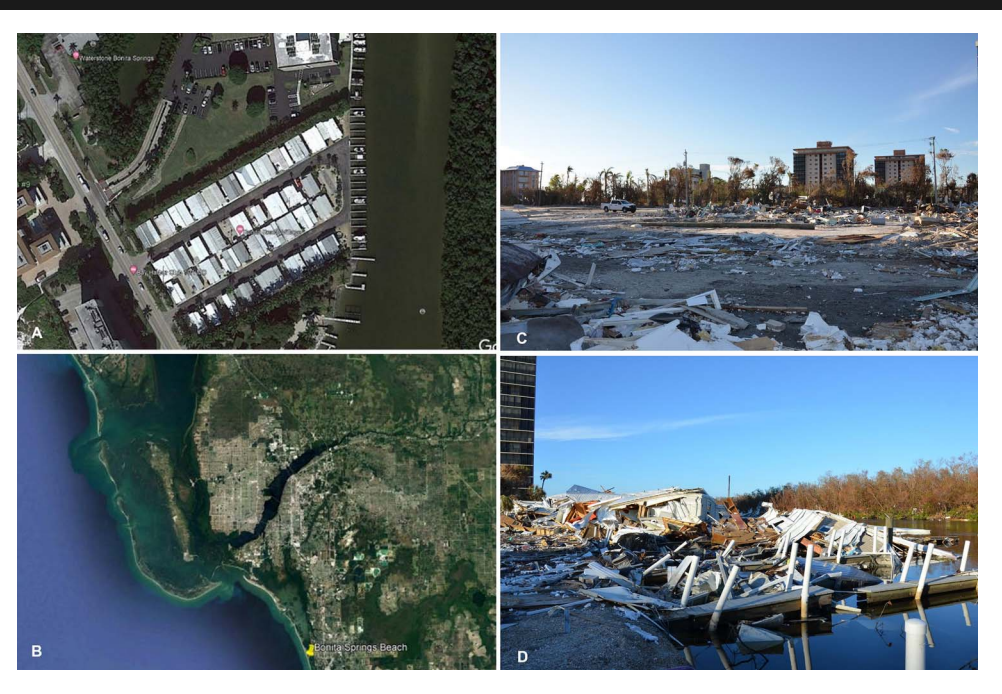


Figure 9. Complete destruction of a mobile home community. (A) Aerial view of a community with 38 waterfront mobile homes before Hurricane Ian. (B) Location of the mobile home community along the landward side of the barrier island where Bonita Springs Beach is located (pin drop at the bottom). Google Earth photo was taken in 2021. (C) All the 38 mobile homes were completely destroyed. Photo was taken looking north from the south end of the community. (D) Almost all the mobile homes were washed into the estuary and the associated mangrove forest. Photo was taken looking east (landward) from the east edge of the community.

illustrates an example of an older, highly elevated building. This building was deemed destroyed, as indicated by the red poster on the middle piling. One of the oceanfront pilings fell over. Similar to the above case of a newer building, everything on the nonliving first floor was washed away, leaving many dangling cables and destroyed fences. A couple of buildings seaward were washed away, leaving empty pilings. Figure 13C illustrates two examples of multistory buildings. The building to the right fared unusually well, with almost everything appearing to be intact, even the screens on the patios. The building to the left was not elevated as high. The first living floor appears to be severely damaged with two patio decks washed away. Modest damage to the patio screens on higher floors occurred, likely by wind forcing. It is worthy of note that palm trees are quite resilient, and most remained upright, even when nearly 1 m of the root system was scoured out (Figure 13C, left edge). Figure 13D illustrates an example of a nonelevated single-story gift shop along the landward side of the main road on Ft. Myers Beach. The building was destroyed, as marked by the red poster next to the flag. It is apparent that the waves were still quite high at this location, which is over 130 m from the Gulf of Mexico shoreline. The shredded and dangling insulation materials from the ceiling were likely caused by waves crashing at the ceiling. The air-conditioning units on the roof remained, in contrast to the two other single-story examples (Figure 13A, B), where the air-conditioning units washed away along with other appliances were likely on the nonliving first floor.

In summary, the widespread damage by Hurricane Ian was controlled by the extremely energetic forcing exerted on the expansive low-lying and often densely developed environment. This particular combination of forcing mechanism and receiving environment resulted in widespread destruction of the built environment. Furthermore, the non-biodegradable and harmful artificial materials that were washed away from the developed areas were distributed broadly into the pristine environments. It is not clear how the debris that has sunk to the bottom of the shallow estuary or become trapped in the mangrove islands can be removed.

Hurricane Ian-Induced Beach and Dune Changes

The high storm waves superimposed on the elevated water level caused widespread beach and dune erosion along the barrier islands. Based on different morphological responses of barrier islands to storm impacts, Sallenger (2000) developed four impact scales, including swash regime, collision regime, overwash regime, and inundation regime. For the case of Hurricane Ian's impact along the southwest Florida coast, all the barrier islands shown in Figure 2D were impacted by an overwhelming inundation regime. The spatial patterns of the beach-dune changes were well captured by the pre- and poststorm airborne LIDAR surveys. It is important to point out that airborne LIDAR surveys often cannot reliably capture the elevation of the subaqueous portion of the profile, particularly within the surf zone, where significant changes occur. Similar limitations of airborne LIDAR surveys were observed for the pre- and poststorm surveys before and after Hurricane Micheal in 2018 (Wang et al., 2020). Here, the analysis was focused on the subaerial portion of the beach and the dunes.



Figure 10. Numerous non-biodegradable and harmful materials were washed into Charlotte Harbor and associated mangrove forest. (A) An entire house was washed into the estuary. (B) A small mangrove island was severely damaged with a storage tank and various, mostly plastic, debris. (C) A large amount of debris from the mobile home community, as shown in Figure 9, was washed into a mangrove forest. (D) Efforts to remove the debris. The upper limit of the debris indicates the level of storm surge. All photos were taken landward of developed barrier islands.

The main goal here is to discuss patterns of beach and dune changes under different local settings, e.g., pristine or developed with various degrees of intensity and pattern. Systematic assessment of beach-dune volume changes induced by Hurricane Ian was provided by Clark, Murshid, and Weeks (2023). It is worth noting that the term "dune" is used rather generally here to indicate vegetated back-beach areas. The vegetation ranges from grass type to high and dense trees and/or bushes. Strictly speaking, these are not eolian dunes because the sediments are dominantly poorly to moderately sorted shelly sand as opposed to well-sorted windblown fine sand. They also do not demonstrate the typical dune morphology. From a sediment transport point of view, the features referred to as dunes in this paper were not formed by the accumulation of windblown sand. The generally ridge-shaped and coarse shelly sand suggests that these features are more likely old beach ridges that became vegetated. Sometimes, a thin, typically less than 10 cm, layer of well-sorted, fine, windblown sand was observed at the surface. The lack of tall eolian sand dunes is consistent with the lowwind and humid nature of the southwest Florida coast, in addition to the high rate of shell production. Nevertheless, the terms "dune" and "dune field" are used in this paper to separate the vegetated area with slightly higher elevation from the sandy beach seaward.

Figure 14 illustrates two representative examples of beachdune changes along mostly pristine sections of the barrier islands. Figure 14A-C is an example from Sanibel Island (Figure 2C). Significant beach and dune erosion occurred within roughly 50 m from the shoreline, with up to 1 m elevation loss. Little morphology change occurred in the densely vegetated area. Ground observations indicate that the dense vegetation significantly prevented bed scouring, as well as limiting the penetration of overwash deposits. Wang and Horwitz (2007) observed similar limitation imposed by dense vegetation on the patterns of storm-induced beach-dune erosion and overwash along the southeast Florida Atlantic coast by Hurricanes Frances and Jeanne in 2004. Figure 14B-D illustrates another example with the dense vegetation located further inland. In this case, the airborne LIDAR captured subaqueous changes to roughly 1 m below MSL. Beach recovery in the form of ridge-andrunnel development was measured at this location within 2 weeks after the storm. Development of ridge and runnel features, as a

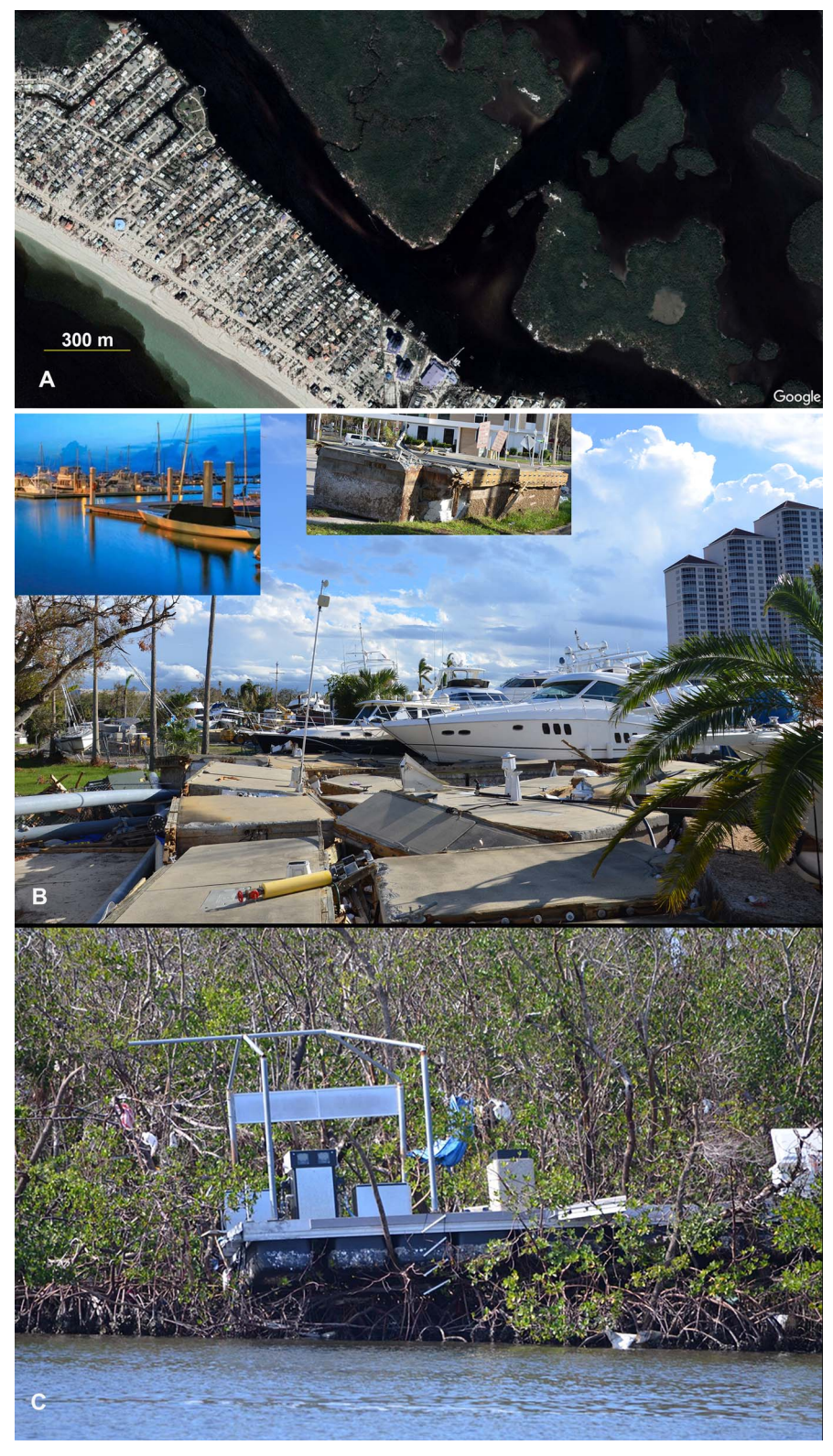


Figure 11. Widespread artificial debris generated by Hurricane Ian. (A) The amount of non-biodegradable and harmful debris washed into the mangrove islands within Charlotte Harbor is closely related to the nearby heavily developed areas; example is from Estero Island (aka Ft. Myers Beach). (B) The high storm surge exceeded height of the anchor pilings of a marina, resulting in all the vessels being washed on land; example is from downtown Ft. Myers. (C) A section of a floating dock and associated fuel station was washed into a mangrove island; example is from southern Estero Bay. See Figure 2 for general locations.



Figure 12. Numerous non-biodegradable and harmful materials were washed into interior wetlands of a barrier island. Example here is from Barefoot Beach in Bonita Springs (Bonita Beach area in Figure 2). The upper limit of the debris indicates the level of storm surge.

morphological indicator of immediate poststorm beach recovery through natural processes, was also observed by Wang *et al.* (2006) along the northwest Florida coast and by Roberts, Wang, and Puleo (2013) along the Delaware Atlantic coast. An elevation loss of up to 1 m was also measured at this location. Overwash deposits were measured across a roughly 40-m-wide area with relatively sparse vegetation and terminated in the area with dense vegetation (Figure 14C, D).

Figure 15 illustrates two examples from developed sections of the barrier islands. In both cases, the single-family residential buildings are located relatively far, or over 100 m, from the Gulf of Mexico shoreline with dense vegetation in front. The Estero example (Figure 15A, C) from Ft. Myers Beach (Figure 2B) included a subaqueous portion of up to 1 m below MSL. The ridge and runnel feature, indicating poststorm beach recovery, was also measured. The nearly 2-m-high narrow dune less than 10 m in width was eroded. The dense vegetation landward limited both erosion and overwash deposition. Similar morphological change was measured at the Sanibel example (Figure 2C), where the dense vegetation is closer to the shoreline (Figure 15B, D).

Figure 16 illustrates two examples from densely developed sections of the barrier islands. Different from the above examples, the buildings are multistory, very close to the shoreline, and with a seawall along the ocean side. For the Naples example (Figure 16A, C; see also Figure 2D), both the beach and the dune, likely artificial based on shape and elevation, were eroded. The manicured ground-cover vegetation landward of the seawall suffered some erosion. The scour ditch in front of the seawall was slightly over 1 m deep. For the Bonita example (Figure 16B, D; see also Figure 2D), the beach and the artificial dune (based on the regular vegetation pattern) were eroded. The scour ditch in front of the seawall was also about 1 m deep. Ridge and runnel features were also developed at these two locations directly after the storm. The low artificial dunes along these narrow prestorm

beaches were not adequate to provide any protection against the overwhelming Hurricane Ian surge at these two locations.

Numerous gullies were observed in the poststorm aerial photos (Figure 17E, F) and on the ground (Figure 6D). Based on the shape and shore-perpendicular orientation of the gullies, they are interpreted as being formed by channelized seaward flow during the subsidence of the storm surge. As apparent from the aerial photos, many gullies were associated with dune overwalks. As a matter of fact, the three examples here (Figures 6D 17E, F) are all related to dune overwalks. It is likely that the dune overwalks created a favorable condition to channelize seaward flow as the storm surge subsided. More specifically, as illustrated in Figure 6C, D, the gully developed along the left side of the dune overwalk, where there was no vegetation before the storm. In other words, it is likely the influence of the dune overwalk on local vegetation that initiated the gully, as opposed to the structure itself. This channelized seaward flow was apparently strong enough to scour the prestorm beach and dune. For the two examples shown in Figure 17B, D, the bottom of the gully was slightly (~0.1 m to 0.2 m) above NAVD88 zero, or at about mean high tide. This further confirms the interpretation that the scour occurred mostly when the water level was above mean high tide, or during the receding storm surge.

In summary, the prestorm beaches and dunes in the study area were mostly lower than 2 m NAVD88. In addition, morphology-wise, there was no distinctive boundary between the beach and the dune field, e.g., shape and significant increase in elevation. This is consistent with the fact that the so-called dunes were mostly vegetated old beach ridges with minor contributions from windblown sand. The low beach and dune system was submerged under up to 2 m water depth during the peak period of the storm. The entire dune field was too low to offer any protection against Hurricane Ian's storm surge. Although it did not stop the landward penetration of the storm surge, the dense and tall tree-type vegetation played a significant









Figure 13. Damage to beachfront buildings. All examples are from the very densely developed Ft. Myers Beach (Figure 2B for location). (A) A relatively new single-family house on concrete pilings. The house to the left on wood piling was washed away. (B) An older single-family house on

role in controlling the landward limit of erosion, as well as deposition by overwash.

Beach and Dune Volume Change Caused by Hurricane Ian

A major advantage of the airborne LIDAR surveys is the dense and continuous spatial coverage. This allows accurate computation of volume change and its longshore variation, particularly over the subaerial portion of the barrier islands. The goal here was not to quantify the volume change along the entire barrier-island chain caused by Hurricane Ian, which can be found in Clark, Murshid, and Weeks (2023). Instead, like the above discussion on profile changes, the following volume-change discussion focused on the magnitude and spatial pattern of the changes associated with different local coastal settings, e.g., along pristine or heavily developed sections. Examples from three barrier islands are illustrated and discussed here, including, from south to north, Barefoot Beach Island (Bonita Beach), Estero Island (aka Ft. Myers Beach), and Sanibel Island (Figure 2).

The Barefoot Beach example (Figure 18) spans a 2 km section of beach with a pristine beach-dune system along the southern portion shifting to a developed stretch along the northern portion. Overall, the net volume loss ranged from 8 to 19 m³/m, with a northward increasing trend. The magnitudes of the volume loss are modest compared to those measured, e.g., along the northwest Florida coast after Hurricane Ivan in 2004 (Wang et al., 2006) and after Hurricane Michael in 2018 (Wang et al., 2020). The relatively small volume loss was controlled by the much lower elevation of the beach and dune system, as compared to those along the northwest Florida coast (Claudino-Sales, Wang, and Horwitz, 2008, 2010; Houser and Hamilton, 2009; Houser, Hapke, and Hamilton, 2008). The fact that both the beach and dune were deeply inundated at the peak of the storm might have limited the erosion by wave forcing. Along the mostly pristine section (Figure 18A,B,D), the beach-dune change was rather uniform alongshore. Slight volume gain was measured near the shoreline, likely related to the growth of the ridge and runnel features, as observed in all the example profiles discussed above. Most of the volume loss occurred in the transition zone between the beach and the dune field. The densely vegetated dune field gained some sand in the form of washover. An example along the developed section, with high-rise buildings, is shown in Figure 18E,C. Compared to the pristine section, more alongshore variation was measured, including two gullies (Figure 18F). The interaction between the buildings and the flow field associated with the receding storm surge likely controlled the locations of the gullies. Along this developed section, the vegetation was trimmed (Figure 18C). The thicker overwash deposit, as compared to the section with tall trees (Figure 18B), was likely influenced by the reduced blocking ability by the lower vegetation. The general magnitude

tall concrete pilings. Nearby houses on pilings were washed away. (C) Multistory buildings: The building that is elevated higher (right) appears to have fared better than the one that is elevated lower (left). (D) Unelevated single-story shop that was completely destroyed.

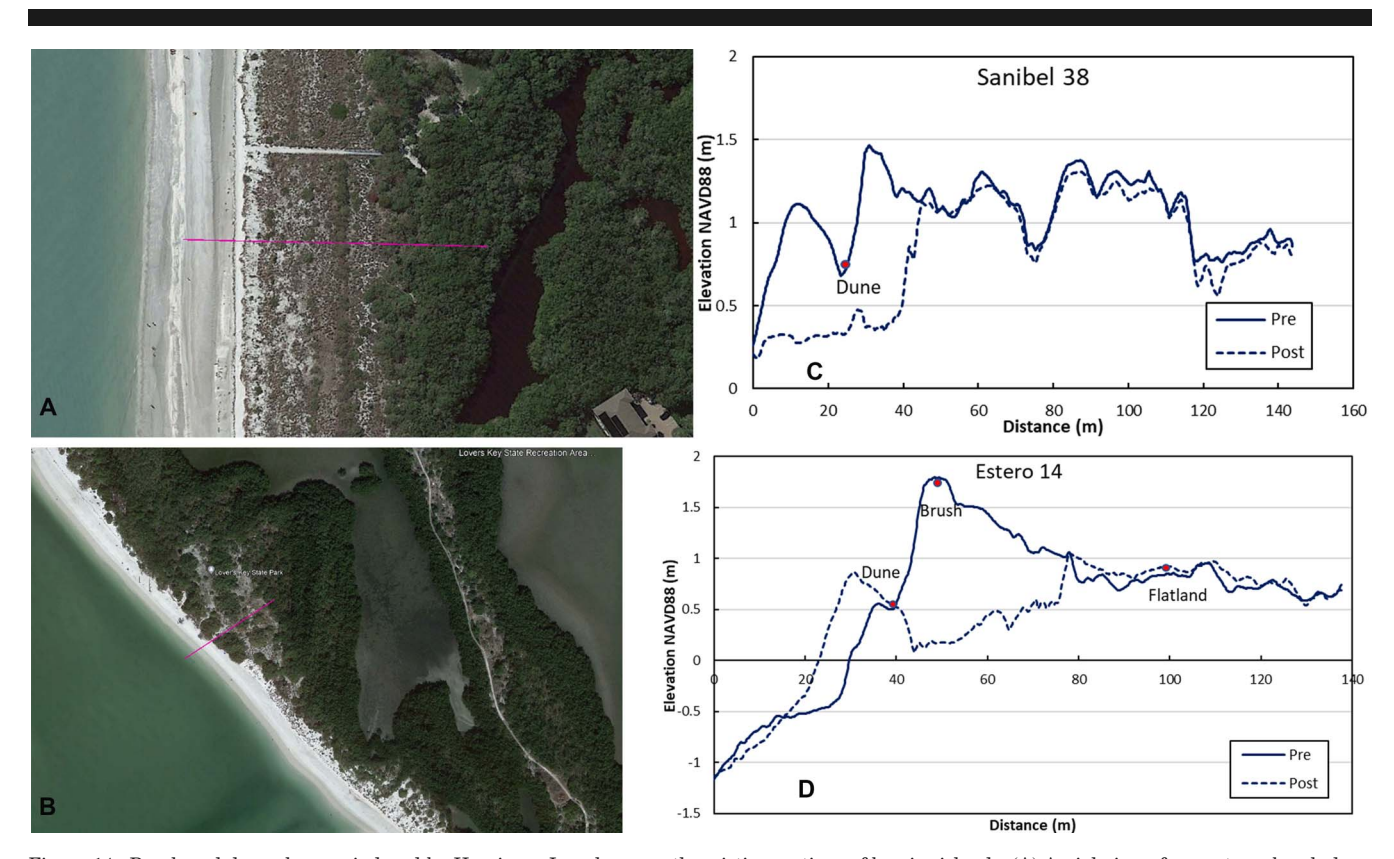


Figure 14. Beach and dune changes induced by Hurricane Ian along mostly pristine sections of barrier islands. (A) Aerial view of a prestorm beach-dune system at Sanibel Island (Figure 2C for location). (B) Aerial view of a prestorm beach and dune system at Lover's Key State Park (the island to the south of Ft. Myers Beach; see Figure 2B for location). (C) Pre— and post—Hurricane Ian beach-dune profiles at panel A location (purple line). (D) Pre— and post—Hurricane Ian beach-dune profiles at panel B location (purple line). The label "Dune" indicates the seaward edge of the dune field as identified from the aerial photo. Beach profiles were extracted from the airborne LIDAR data from the U.S. Army Corps of Engineers and FDEP.

of the volume changes as discussed above is comparable to the values obtained by Clark, Murshid, and Weeks (2023) for this stretch of the coast.

Figure 19 illustrates examples from the very densely developed Estero Island, aka Ft. Myers Beach (Figure 2C). Three sections with a relatively wide pre- and poststorm beach were selected. Figure 19B illustrates an example near the southern and accretionary end, where a spit was developing before the storm. Considerable sediment was washed into the shallow pond, almost balancing the erosion at the beach and resulting in a small net change of 3.4 m³/m. Figure 19D (cf. Figure 19A, D) represents a rather unusual case with a very wide, low, and flat beach without any vegetation. The wide and flat beach received modest sedimentation, likely from the beach erosion seaward. The overwash, which was also observed during field investigations, combined with the growth of ridge and runnel features near the shoreline balanced the erosion, resulting in minimal net change. Figure 19C differs from Figure 19D in that there is a wide and vegetated dune field, although with low elevation. The low dune field was eroded by the storm, resulting in the largest net volume loss of 23.3 m³/m along the seven studied sections along Ft. Myers Beach (red boxes in Figure 19A). The unvegetated paths through the dune field, identifiable from Figure 19A, led to the formation of gullies, confirming the interpretation that the barren path provided a favorable condition for channelizing flow driven by the receding storm surge. The seven studied sections did not reveal any spatial trend in the volume changes. The overall magnitude of the volume changes as discussed above is comparable to the values obtained by Clark, Murshid, and Weeks (2023) for this stretch of the coast.

Figure 20 illustrates several examples along the southward-facing broad headland on Sanibel Island. Among the eight barrier islands shown in Figure 9B, this represents the widest section. This part of the coast also had the most gullies. The majority of dune overwalks and/or unvegetated pathways through the dunes turned into gullies, suggesting a rather reliable causal relationship. These gullies led to substantial longshore variation of volume change, while the alongshore-averaged volume changes (Figure 20A) are comparable to the sections without gullies (Figures 18A and 19A). Furthermore, the general pattern was similar to the other two barrier islands and included (1) small gains near the shoreline due to the formation of ridge and runnel features, (2) erosion along the back beach and frontal dunes, and (3) overwash deposition landward. Despite the shoreline orientation change around the broad headland and the gullies, the volume change averaged over each section at the six studied sections remained rather consistent (Figure 20A).

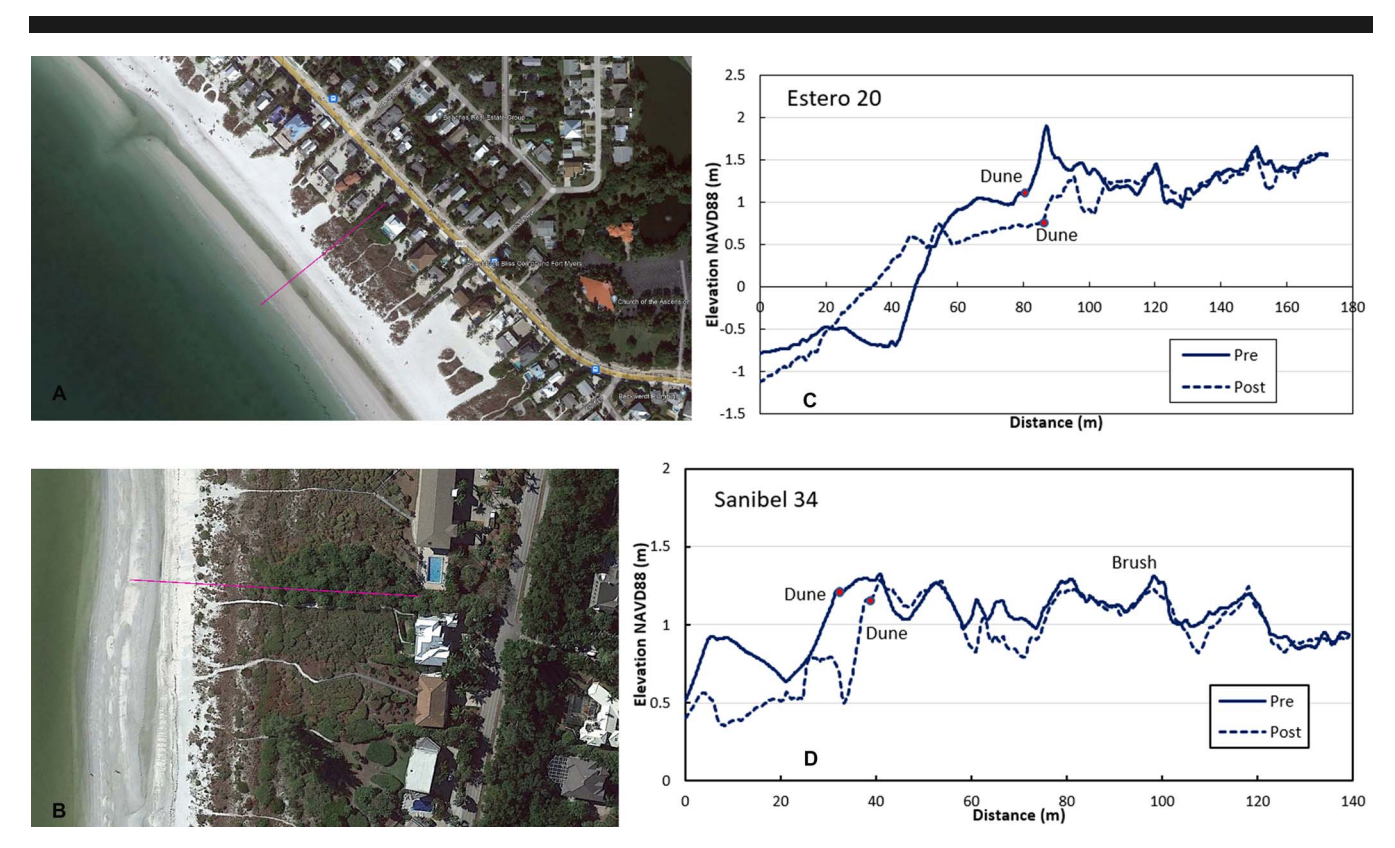


Figure 15. Beach and dune changes induced by Hurricane Ian along developed barrier islands. (A) Aerial view of a prestorm beach-dune system at Estero Island, aka Ft. Myers Beach (Figure 2B for location). (B) Aerial view of a prestorm beach and dune system at Sanibel Island (Figure 2C for location). (C) Pre— and post—Hurricane Ian beach-dune profiles at panel A location (purple line). (D) Pre— and post—Hurricane Ian beach-dune profiles at panel B location (purple line). The label "Dune" indicates the seaward edge of the dune field as identified from the aerial photo. Beach profiles were extracted from the air-borne LIDAR data from the U.S. Army Corps of Engineers and FDEP.

In summary, the magnitudes of beach-dune volume change as caused by Hurricane Ian along the southwest Florida coast were small as compared to storm-induced changes along other coasts. This was likely controlled by the overall low elevation of the beaches and dunes, which led to deep inundation at the peak of the storm. Furthermore, the volume change per unit length was rather similar, ranging from 10 to 25 m³/m at three barrier islands spanning over 40 km of the studied coastline. The gaps in dune vegetation, whether caused by dune overwalks or barren paths, were reliably related to the formation of gullies. Ground observations also revealed extensive damage to vegetation due to strong wind and submergence by seawater (Figures 6D, 9D, 10B, C, D, 12, and 18B, C).

DISCUSSION

The concepts of "Working with Nature" (PIANC, 2011), "Engineering with Nature (EWN)" (Bridges et al., 2014a), and Nature-Based Solutions (NBS) (Cohen-Shacham et al., 2016, 2019; IUCN, 2022) have been applied increasingly in recent years to build resiliency in coastal areas against sealevel rise and storm impacts. Bridges et al. (2014b) introduced the general approach of natural and nature-based features (NNBF) for EWN. Based on Bridges et al. (2014b), natural

features (NF) are created and evolve over time through the actions of physical, biological, geological, and chemical processes operating in nature, while nature-based features (NBF) are those that may mimic characteristics of natural features but are created by humans to provide specific services. Within the NNBF paradigm, beaches, dunes, and mangrove forests are considered natural features, while nourished beaches and dunes and restored mangrove habitat are considered nature-based features. Coastal resiliency improvement adopting EWN or NBS often emphasizes innovative application of NNBF (Bridges et al., 2014a; IUCN, 2022). Specific to resiliency against storm impacts on barrier island and estuary environments, various studies have examined the functions of beaches, dunes, oyster reefs, and dense vegetation. Wamsley et al. (2009a, 2009b, 2010) examined the potential of wetlands in reducing storm surge and storm waves based mostly on numerical modeling. Narayan et al. (2016) and Reguero et al. (2018) reviewed the effectiveness of NNBF, such as oyster reefs or mangrove habitat, in reducing wave energy based on field measurements. The specific environmental characteristics of the Charlotte Harbor area as discussed above combined with the extensive field data collected during the passage of Hurricane Ian provide an insightful case to examine the effects of NNBF on reducing storm waves and surge. It is worth noting that

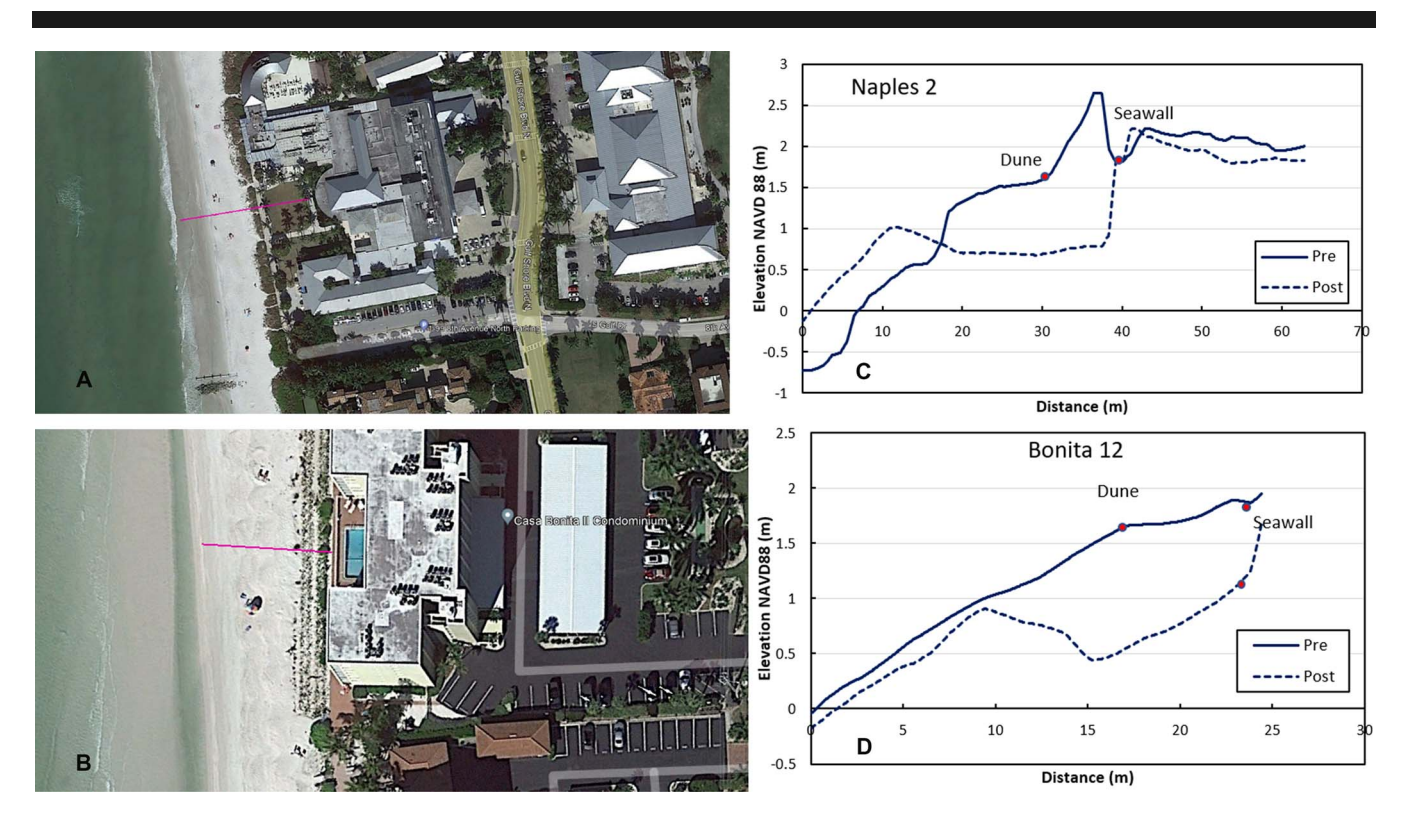


Figure 16. Beach changes induced by Hurricane Ian along sections backed by a seawall. (A) Aerial view of a prestorm beach at Naples (Figure 2D for location). (B) Aerial view of a prestorm beach at Bonita Beach (Figure 2D for location). (C) Pre—and post—Hurricane Ian beach-dune profiles at panel A location (purple line). (D) Pre—and post—Hurricane Ian beach-dune profiles at panel B location (purple line). The label "Dune" indicates the seaward edge of the dune field as identified from the aerial photo. Beach profiles were extracted from the airborne LIDAR data from the U.S. Army Corps of Engineers and FDEP.

Hurricane Ian is an extremely energetic and rare case and may not represent the NNBF functions under typical storm conditions.

The relevant NNBF features here include, from seaward to landward: (1) a nearshore berm placement (NBF) (Brutsche and Pollock, 2017; Brutsche *et al.*, 2014); (2) sandy beaches, both natural (NF) and nourished (NBF); (3) dunes, mostly natural (NF); and (4) mangrove forests within barrier island interiors and on islands in Charlotte Harbor, mostly natural (NF). Except the top of the mangrove forests, all these features were submerged by the storm surge induced by Hurricane Ian.

Wave-height reduction by the above NNBF was not directly measured. The nearshore berm that was studied by Brutsche et al. (2014) had equilibrated to the background profile and should not have induced any spatial variation on wave propagation during Hurricane Ian. Wave height at the boundary between beach and dune at a Sanibel Island location was measured by a USGS rapid deployment gauge (Figure 6). However, the spatial coverage was not adequate to quantify wave reduction by the beach and dune features. Based on the extensive and severe physical damage of buildings landward of beaches and dunes (Figures 9 and 13), it is reasonable to deduce that the wave-height reduction by the deeply submerged low beachdune system was not enough to provide significant protection of the infrastructure landward. Although dense vegetation did not

fundamentally prevent storm surge from propagating through, it appears to have significantly reduced the magnitude of sediment transport and limited the landward penetration of erosion, as well as overwash deposition (Figures 14, 15, and 17). The example at Barefoot Beach (Figure 18) illustrates that tall and dense vegetation (Figure 18B,D) was more effective in reducing both erosion and overwash deposition as compared to the artificially trimmed vegetation (Figure 18C,E). Trimming tall trees and artificially hindering dune growth, e.g., by raking the beach to prevent vegetation from being established, are fairly common practices along developed beaches to ensure an unobstructed ocean view. Damage by Hurricane Ian demonstrates that these practices can weaken protections against wave forcing.

The extensive spatial coverage of the water-level measurements (Figures 5, 6, and 7) provides valuable data to examine the effects of NNBF in reducing storm surge at a regional scale, particularly at the extremely elevated water level in this case. The relevant features include barrier islands with different orientations and widths bordering the estuary and numerous islands of various sizes within the estuary. At a regional scale, the influence of the barrier islands and islands within the estuary on the spatial distribution of storm surge cannot be identified from the contour map of the high-water mark (Figure 7), representing maximum storm surge level. As a matter of fact, the surge level was higher landward of Pine

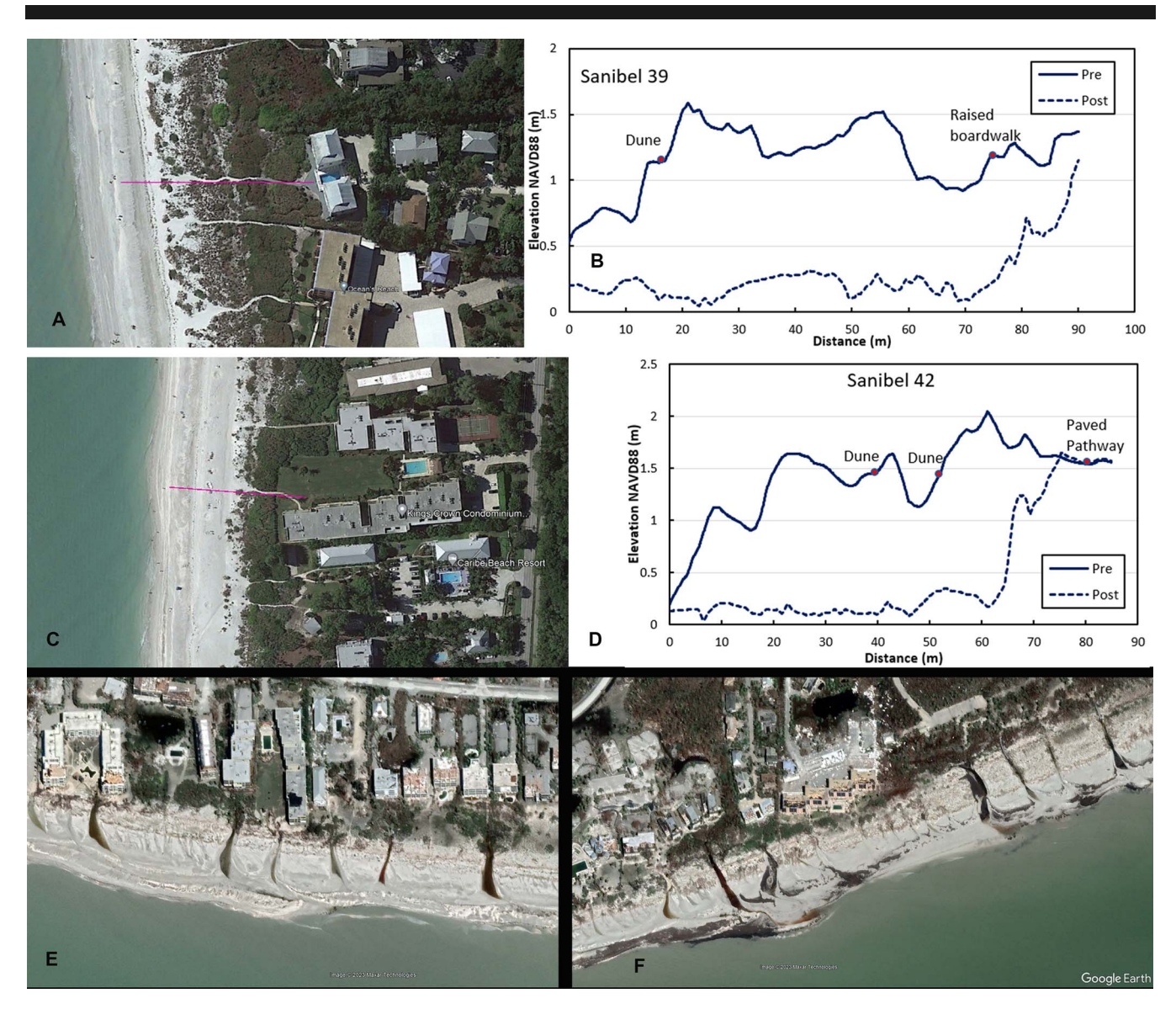


Figure 17. Beach and dune changes induced by Hurricane Ian along developed sections of Sanibel Island (Figure 2C for location). (A) Aerial view of a prestorm beach-dune system. (B) Pre– and post–Hurricane Ian beach-dune profiles at panel A location (purple line). (C) Aerial view of a prestorm beach and dune system. (D) Pre– and post–Hurricane Ian beach-dune profiles at panel C location (purple line). The label "Dune" indicates the seaward edge of dune field as identified from the aerial photo. (E) Poststorm view of the location shown in panel A; note the many gullies cut through the dune and beach area. (F) Poststorm view of the location shown in panel B; note the many gullies cut through the dune and beach area. Beach profiles were extracted from the airborne LIDAR data from the U.S. Army Corps of Engineers and FDEP.

Island, the largest island by far in Charlotte Harbor. This suggests that the friction exerted by the landforms should be secondary to the forcing, from the southwest in this case, in surge generation or dissipation.

Figure 21 illustrates a transect crossing a heavily developed barrier island (Ft. Myers Beach), a heavily developed estuarine island (San Carlos Island), and a dredged marina developed on the mainland shoreline. At the seaward-most location along the open Gulf of Mexico coast, the peak surge was 13.2 ft (4.0 m) NAVD88. Landward of the barrier island, the peak surge was 12.1 ft (3.7 m) NAVD88. The slightly lower surge on

the landward side, as compared to that along the seaward side, may have been caused by the lack of wave setup instead of by friction over the barrier island. The unfiltered water level likely reflects wave influence reaching 15.6 ft (4.8 m) along the Gulf of Mexico side. The peak surge at the landward side, about 0.7 km from the seaward gauge, occurred about 27 minutes after the peak at the Gulf of Mexico side. Approximately 2.5 km further inland, at the landward edge of a dredged waterfront community, the peak surge as determined based on the high-water mark was 12.3 ft (3.8 m) NAVD88. This is roughly the same as that measured at the seaward side of a wide developed mangrove island,

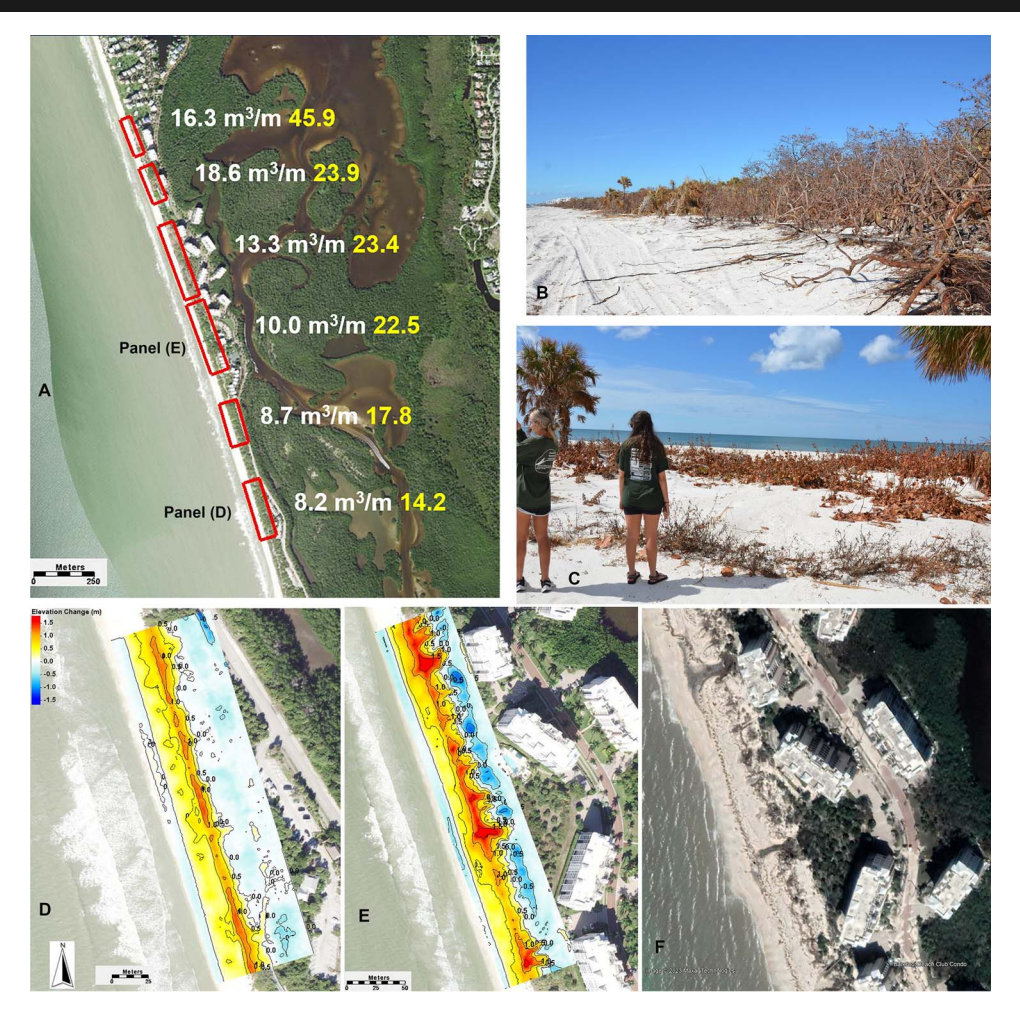


Figure 18. Beach and dune volume changes induced by Hurricane Ian along a section of Bonita Beach (Figure 2D for location). (A) Aerial view of the prestorm beach-dune system along an approximately 2 km section of beach. The white numbers indicate net volume loss combining both erosion and deposition. The yellow numbers indicate only the eroded volume. Each number represents volume change per unit alongshore length averaged over the corresponding red box. (B) Poststorm ground view looking south at panel D; note that beach repair had started about 1 month after the storm. (C) Poststorm ground view looking seaward at panel E. (D) Elevation change, where warm red colors (positive values) indicate erosion, while cool blue colors (negative values) indicate deposition. Location is marked in panel A, representing a mostly undeveloped section. (E) Elevation change, where warm red colors (positive values) indicate erosion, while cool blue colors (negative values) indicate deposition. Location is marked in panel A, representing a developed section backed by high-rise buildings. (F) Poststorm aerial view of location shown in panel E; note the two gullies cut through the dune and beach area. The volume-change calculation was based on the airborne LIDAR data from the U.S. Army Corps of Engineers and FDEP.

suggesting minimal friction-induced surge dissipation. Overall, negligible storm surge reduction was measured over a 3.2 km distance across a barrier island and a large island, although both are heavily developed. Due to the heavily developed nature of the southwest Florida coast, measurements along pristine section were limited. However, there is no reason to believe that dense natural vegetation would exert much stronger overall friction than dense buildings plus landscapes, for the reduction of storm surge height.

Lessons Learned Concerning Coastal Management and Resiliency Building

Based on the findings by Palm and Bolsen (2023), it is more likely than not that the low-lying southwest Florida area will continue to grow at a rapid pace despite the catastrophic

impact of Hurricane Ian, in addition to longer-term risks associated with rising sea level. Some anecdotal observations of poststorm recovery efforts support this assessment. Therefore, better preparations to minimize long-term damage to both built and natural environments are crucial. Here, lessons learned from the post–Hurricane Ian observations are discussed.

Mobile homes are clearly not capable of withstanding hurricane-strength forcing in terms of wind, surge, or waves. They simply should not be placed close to the ocean. In addition to being destroyed, they also served as the sources of numerous non-biodegradable materials that were washed into sensitive estuarine habitats. However, as its name suggests, mobile homes should have the advantage of being readily moved out of harm's way. That was not the case during the passage of Hurricane Ian. Therefore, in addition to ordering evacuation of mobile homes



Figure 19. Beach and dune changes induced by Hurricane Ian along Estero Island, aka Ft. Myers Beach (Figure 2B for location). (A) Aerial view of the prestorm beach-dune system. The white numbers indicate net volume loss combining both erosion and deposition. The yellow numbers indicate only the eroded volume. Each number represents volume change per unit alongshore length averaged over the corresponding red box. (B) Elevation change, where warm red colors (positive values) indicate erosion, while cool blue colors (negative values) indicate deposition. Location is marked in panel A, representing a section with a large setback before the development. (C) Elevation change, where warm red colors (positive values) indicate erosion, while cool blue colors (negative values) indicate deposition. Location is marked in panel A, representing a section with relatively wide and low dunes. (D) Elevation change, where warm red colors (positive values) indicate erosion, while cool blue colors (negative values) indicate deposition. Location is marked in panel A, representing a section with a wide and flat beach with no vegetated dunes. The volume-change calculation was based on the airborne LIDAR data from the U.S. Army Corps of Engineers and FDEP.

when hurricane impact becomes imminent, some sort of medium-term preparation plan, *e.g.*, at the beginning hurricane season, should be developed to prevent the pollution of the larger environment. Another potential advantage of mobile homes is that they are less costly and can be repaired relatively quickly. This should also be considered during the prestorm preparation.

Elevating a building, a single-story or a high-rise structure, has been an effective way of staying above a certain storm surge level. However, as illustrated by the examples in Figure 13, elevation is just one of the factors that determine the buildings' ability to sustain storm impact. It is beyond the scope of this paper to systematically discuss the structural integrity of elevated buildings. However, the first floor is almost always used: as a parking garage, as a space for various utilities, and/or for general storage. Significant portions of the materials stored on this nonliving floor were washed out by Hurricane Ian and distributed broadly into sensitive habitats. Therefore, prevention or reduction of the damage to the often-costly items on the first floor and subsequent

ejection of these items into sensitive environments should be considered as essential parts of storm preparation. Ideally, this surge-vulnerable floor should not be used to store materials or appliances that cannot be readily removed.

A rather remarkable impact by Hurricane Ian is the wide-spread distribution of non-biodegradable artificial materials within a variety of sensitive environments, including mangrove islands (Figures 9D, 10B, C, D, and 11A, C), barrier island interior wetlands (Figures 8A and 12), and the broad estuary waterbody (Figures 9D and 10A). Large amounts of debris were also distributed within downtown Ft. Myers (Figures 8C and 11B). It is worth noting that Figures 10A and 9D illustrate examples of materials within the estuary waterbody that extended above water. Numerous pieces of submerged debris were observed over a large area during the field investigations. Sunken debris is visible in Figure 9D. While some of the debris likely resulted from destruction by the strong wave forcing, *e.g.*, the shredded insulation materials from ceilings (Figures 8A, 9C, D, and 13A, B, D), it can be argued that significant portions of the materials,



Figure 20. Beach and dune changes induced by Hurricane Ian along the S-facing section of Sanibel Island (Figure 2C for location). (A) Aerial view of the prestorm beach-dune system. The white numbers indicate net volume loss combining both erosion and deposition. The yellow numbers indicate only the eroded volume. Each number represents volume change per unit alongshore length averaged over the corresponding red box. (B) Elevation change, where warm red colors (positive values) indicate erosion, while cool blue colors (negative values) indicate deposition. The location is marked in panel A, representing a section of beach facing SW. (C) Elevation change, where warm red colors (positive values) indicate erosion, while cool blue colors (negative values) indicate deposition. The location is marked in panel A, representing a headland section facing roughly S-SW. (D) Elevation change, where warm red colors (positive values) indicate erosion, while cool blue colors (negative values) indicate deposition. The location is marked in panel A, representing a section of beach facing S-SE. The volume-change calculation was based on the airborne LIDAR data from the U.S. Army Corps of Engineers and FDEP.

e.g., single-use plastics (Figures 10B, C, D and 12), storage tanks (Figure 10B), and numerous household appliances (air-conditioning units and water heaters, etc.), can be better controlled through simple preparation. For example, plastics should be more securely stored to prevent them from being washed or blown away. Household appliances, if placed on the nonliving first floor of elevated buildings, should be anchored more securely. It would not make much sense if a building is elevated to avoid the first floor being flooded by storm surge, while in the meantime, it is being used for almost everything ranging from costly essential appliances to general storage. At the very least, the materials on the flood-prone lower floor should be adequately anchored to prevent them from being washed into sensitive environments.

Numerous vessels with a wide range of sizes suffered anchor failure and were washed on land (Figure 11B) or into mangrove habitat (Figure 11,C). Although there were various causes of anchor failure, we identified one common cause relating to floating docks. Floating docks are commonly used in southwest Florida and elsewhere. They rise and fall with tides and provide convenient boat access. However, many of the floating docks failed during Hurricane Ian because the storm surge exceeded the height of the anchor pilings, and the docks simply floated off the pilings. In some cases, although the pilings were taller than the peak surge, they failed to maintain their integrity

against the forcing exerted by the elevated dock and vessels. Tilted anchor pilings were observed during the field investigations. Stronger anchor pilings and more secure design are necessary for floating docks to prevent the entire system from being washed into sensitive environments such as mangrove islands, although damage to the vessels and docks might still occur.

Although the humid weather, generally slow wind speed, and shelly sand are not favorable conditions for dune growth, they are favorable conditions for the development of dense and tall vegetation. Seagrape trees (Coccoloba uvifera) are very common directly landward of the sandy beaches, while mangrove trees are common along the bayside shorelines and on numerous islands. These trees can grow quite tall and block the water view. Therefore, they are often trimmed along developed sections (Figures 6D, 13C, and 18C). Although there are no data indicating that the natural and tall trees reduced Hurricane Ian's storm surge in comparison with the trimmed trees, the tall trees were significantly more effective in limiting the landward penetration of beach/dune erosion and overwash deposits by dissipating wave energy (Figure 18B-E). The measured beach and dune changes largely stopped just landward of the edge of dense and tall vegetation (Figures 14 and 15). It should come as no surprise that trimming trees for less obstructed water view would come at the cost of reduced storm protection in terms of erosion and overwash deposits.

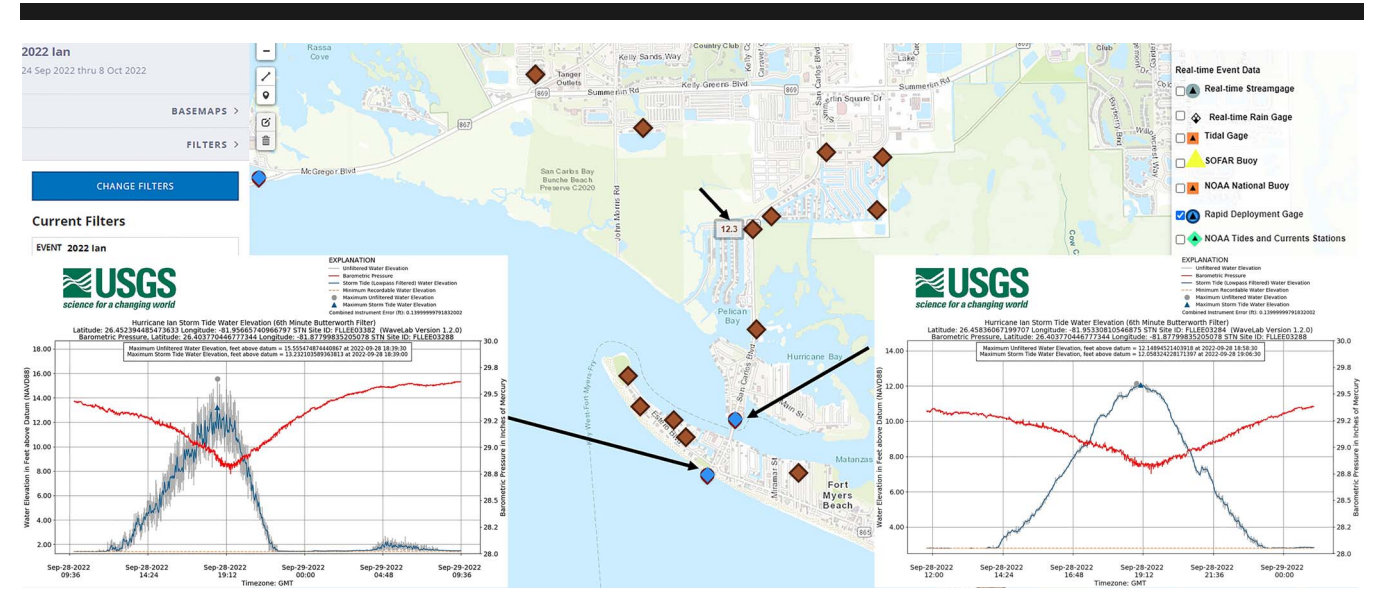


Figure 21. Storm surge levels measured at three locations across Ft. Myers Beach.

CONCLUSIONS

Based on field observations and analysis of a large existing data set, the following conclusions were reached:

- (1) Hurricane Ian induced large-scale inundation in low-lying southwest Florida, submerging all the barrier islands bordering Charlotte Harbor estuary, all the islands within the estuary, and up to 5 km into the mainland.
- (2) Dense and tall vegetation limited the landward penetration of beach-dune erosion and overwash deposition along the barrier islands. Net sand-volume loss from the beach-dune system ranged from 10 to 25 m³/m and was controlled by the deep submergence of the system during most of the storm.
- (3) The extremely high storm surge generated by Hurricane Ian caused severe damage to the built environments over a large area. High storm waves superimposed on the elevated water level contributed to destruction along the barrier islands.
- (4) Hurricane Ian washed a widespread and tremendous amount of non-biodegradable artificial debris into the natural environment, including the numerous estuarine islands, barrier-island interior wetlands, and the estuary waterbody. Measures to prevent materials such as single-use plastics, insulation fibers, and household appliances from being washed into sensitive environments should be significant parts of prestorm preparation.

ACKNOWLEDGMENTS

Travel expenses were partly supported by the National Science Foundation Nearshore Extreme Events Reconnaissance (NEER) program. NEER also provided timely information during and shortly after the storm impact. We are grateful to Lee County and the State of Florida for allowing us to use the one functioning boat ramp to launch our research vessel

shortly after the storm. We thank Tyler Weinard of Lee County for assisting with fieldwork and access. We appreciate the collaboration and discussion with Dr. Tiffany Briggs and her graduate students from Florida Atlantic University during the field investigations.

LITERATURE CITED

AghaKouchak, A; Chiang, F.; Huning, L.S.; Love, C.A.; Mallakpour, I.; Mazdiyasni, O.; Moftakhari, H.; Papalexiou, S.M.; Ragno, E., and Sadegh, M., 2020. Climate extremes and compound hazards in a warming world. *Annual Review of Earth and Planetary Sciences*, 48, 519–548. doi:10.1146/annurev-earth-071719-055228

Beck, T.M. and Wang, P., 2019. Morphodynamics of barrier-inlet systems in the context of regional sediment management, with case studies from west-central Florida, USA. Ocean and Coastal Management, 177, 31–51.

Brecht, H.; Dasgupta, S.; Laplante, B.; Murray, S., and Wheeler, D., 2012. Sea-level rise and storm surges: High stakes for a small number of developing countries. *Journal of Environment & Develop*ment, 21(1), 120–138.

Bridges, T.S.; Lillycrop, J.; Wilson, J.; Fredette, T.; Suedel, B.; Banks, C., and Russo, E., 2014a. Engineering with nature promotes triple-win outcomes. *Terra et Aqua*, 135(June), 17–23.

Bridges, T.S.; Wagner, P.W.; Burks-Copes, K.A.; Bates, M.E.; Collier,
Z.; Fischenich, C.J.; Gailani, J.Z.; Leuck, L.D.; Piercy, C.D.; Rosati,
J.D.; Russo, E.J.; Shafer, D.J.; Suedel, B.C.; Vuxton, E.A., and
Wamsley, T.V., 2014b. Use of Natural and Nature-Based Features
(NNBF) for Coastal Resilience. Vicksburg, Mississippi: U.S. Army
Corps of Engineer Research and Development Center, Technical
Report ERDC SR-15-1, 479p.

Brutsche, K.E. and Pollock C.E., 2017. Strategic Placement of Mixed Sediment in the Form of a Nearshore Berm along Fort Myers Beach, Florida. Vicksburg, Mississippi: U.S. Army Corps of Engineers Research and Development Center, Technical Report ERDC TN-EWN-17-1, 12p.

Brutsche, K.E.; Wang, P.; Beck, T.M.; Rosati, J.D., and Legault, K.R., 2014. Morphological evolution of a submerged artificial nearshore berm along a low-wave microtidal coast, Fort Myers Beach, west-central Florida, USA. *Coastal Engineering*, 91, 29–44.

Bucci, L.; Alaka, L.; Hagen, A.; Delgado, S., and Beven, J., 2023.
National Hurricane Center Tropical Cyclone Report: Hurricane Ian

(AL092022)23–30 September 2022. https://www.nhc.noa
a.gov/data/tcr/AL092022_Ian.pdf

- Bushong, L.C. and Welch, P., 2023. Critical healthcare for older adults post Hurricane Ian in Florida, United States. *Journal of Public Health Policy*, 44(4), 674–684. doi:10.1057/s41271-023-00444-3
- Cheng, J.; Cossu, F.T., and Wang, P., 2021. Factors controlling long-shore variations of beach changes induced by Tropical Storm Eta (2020) along Pinellas County beaches, west-central Florida. Shore and Beach, 89(2), 75–85. doi:10.34237/1008929
- Clark, R.; Murshid, S., and Weeks, G., 2023. Hurricane Ian & Hurricane Nicole Post Storm Beach Conditions and Coastal Impact Report. Tallahassee, Florida: Florida Department of Environmental Protection. https://floridadep.gov/rcp/coastal-engineering-geology/documents/hurricane-ian-hurricane-nicole-post-storm-beach-conditions
- Claudino-Sales, V.; Wang, P., and Horwitz, M.H., 2008. Factors controlling the survival of coastal dunes during multiple hurricane impacts in 2004 and 2005: Santa Rosa barrier island, Florida. Geomorphology, 95(3–4), 295–315.
- Claudino-Sales, V.; Wang, P., and Horwitz, M.H., 2010. Effect of Hurricane Ivan on coastal dunes of Santa Rosa Barrier Island, Florida: Characterized on the basis of pre- and poststorm LIDAR surveys. *Journal of Coastal Research*, 26(3), 470–484.
- Cohen-Shacham, E.; Andrade, A.; Dalton, J.; Dudley, N.; Jones, M.; Kumar, C.; Maginnis, S.; Maynard, S.; Nelson, C.R.; Renaud, F.G., and Welling, R., 2019. Core principles for successfully implementing and upscaling nature-based solutions. *Environmental Science & Policy*, 98, 20–29.
- Cohen-Shacham, E.; Walters, G.; Janzen, C., and Maginnis, S. (eds.), 2016. Nature-Based Solutions to Address Global Societal Challenges. Gland, Switzerland: International Union for Conservation of Nature (IUCN), 97p.
- Davis, R.A., 1994. Barriers of the Florida Gulf Peninsula. In: Davis, R.A. (ed.), Geology of Holocene Barrier Island Systems. Berlin: Springer, pp. 167–206.
- Dawson, R.J.; Khan, M.S.A.; Gornitz, V.; Lemos, M.F.; Atkinson, L.;
 Pullen, J., and Osorio, J.C., 2018. Urban areas in coastal zones. In:
 Rosenzweig, C.; Solecki, W.; Romero-Lankao, P.; Mehrotra, S.; Dhakal,
 S., and Ali Ibrahim, S. (eds.), Climate Change and Cities: Second
 Assessment Report of the Urban Climate Change Research Network.
 New York: Cambridge University Press, pp. 319–362.
- Emanuel, K., 2003. Tropical cyclones. Annual Review of Earth and Planetary Sciences, 31, 75–104.
- Emanuel, K.; Sundararajan, R., and William, J., 2008. Tropical cyclones and global warming: Results from downscaling IPCC AR4 simulations. Bulletin of American Meteorological Society, 89(3), 347–367.
- Gencer, E.; Folorunsho, R.; Linkin, M.; Wang, X.; Natenzon, C.E.; Wajih, S.; Mani, N.; Esquivel, M.; Ali Ibrahim, S.; Tsuneki, H.; Castro, R.; Leone, M.; Panjwani, D.; Romero-Lankao, P., and Solecki, W., 2018. Disasters and risk in cities. *In:* Rosenzweig, C.; Solecki, W.; Romero-Lankao, P.; Mehrotra, S.; Dhakal, S., and Ali Ibrahim, S. (eds.), *Climate Change and Cities: Second Assessment Report of the Urban Climate Change Research Network*. New York: Cambridge University Press, pp. 61–98.
- Grafakos, S.; Pacteau, C.; Delgado, M.; Landauer, M.; Lucon, O., and Driscoll, P., 2018. Integrating mitigation and adaptation: Opportunities and challenges. *In:* Rosenzweig, C.; Solecki, W.; Romero-Lankao, P.; Mehrotra, S.; Dhakal, S., and Ali Ibrahim, S. (eds.), *Climate Change and Cities: Second Assessment Report of the Urban Climate Change Research Network*. New York: Cambridge University Press, pp. 101–138.
- Heidarzadeh, M.; Iwamoto, T.; Šepić, J., and Mulia, I.E., 2023. Normal and reverse storm surges along the coast of Florida during the September 2022 Hurricane Ian: Observations, analysis, and modelling. Ocean Modelling, 185, 102250.
- Houser, C. and Hamilton, S., 2009. Sensitivity of post-hurricane beach and dune recovery to event frequency. Earth Surface Processes and Landforms, 34(5), 613–628.
- Houser, C.; Hapke, C., and Hamilton, S., 2008. Controls on coastal dune morphology, shoreline erosion and barrier island response to extreme storms. *Geomorphology*, 100(3–4), 223–240.

- IPCC (Intergovernmental Panel on Climate Change), 2022. Climate Change 2022: Impacts, Adaptation and Vulnerability. Contribution of Working Group II to the Sixth Assessment Report of the Intergovernmental Panel on Climate Change [Pörtner, H.-O.; Roberts, D.C.; Tignor, M.; Poloczanska, E.S.; Mintenbeck, K.; Alegría, A.; Craig, M.; Langsdorf, S.; Löschke, S.; Möller, V.; Okem, A., and Rama, B. (eds.)]. Cambridge, U.K.: Cambridge University Press, 30560., doi:10.1017/9781009325844
- IPCC, 2023. Climate Change 2023: Synthesis Report. Contribution of Working Groups I, II and III to the Sixth Assessment Report of the Intergovernmental Panel on Climate Change [Core Writing Team, Lee, H. and Romero, J. (eds.)]. Geneva, Switzerland: IPCC, 184p., doi:10.59327/IPCC/AR6-9789291691647
- Irish, J.L.; Resio, D.T., and Divoky, D., 2011. Statistical properties of hurricane surge along a coast. *Journal of Geophysical Research*, 116(C10), C10007. doi:10.1029/2010JC006626
- IUCN (International Union for Conservation of Nature), 2022. Nature-Based Solutions for People and Planet. https://www.iucn.org/theme/nature-based-solutions
- Janssen, M.S.; Lemke, L., and Miller, J.K., 2019. Application of storm erosion index (SEI) to parameterize spatial storm intensity and impacts from Hurricane Michael. Shore & Beach, 87(4), 41–50.
- Karimiziarani, M. and Moradkhani, H., 2023. Social response and disaster management: Insights from Twitter data assimilation on Hurricane Ian. *International Journal of Disaster Risk Reduction*, 95, 103865. doi:10.1016/j.ijdrr.2023.103865
- Kim, S.K., 2020. The economic effects of climate change adaptation measures: Evidence from Miami-Dade County and New York City. Sustainability, 12(3), 1097. doi:10.3390/su12031097
- Knutson, T.R.; McBride, J.L.; Chan, J.; Emanuel, K.; Holland, G.; Landsea, V.; Held, I.; Kossin, J.P.; Srivastava, A.K., and Sugi, M., 2010. Tropical cyclones and climate change. *Nature Geoscience*, 3, 157–163. doi:10.1038/ngeo779
- Lemke, L. and Miller, J.K., 2020. Evaluation of storms through the lens of erosion potential along the New Jersey, USA coast. *Coastal Engineering*, 158, 103699.
- Lin, N.; Emanuel, K.; Oppenheimer, M., and Vanmarcke, E., 2012. Physically based assessment of hurricane surge threat under climate change. Nature Climate Change, 2, 462–467. doi:10.1038/NCLIMATE1389
- McAlpine, S.A. and Porter, J.R., 2018. Estimating recent local impacts of sea-level rise on current real-estate losses: A housing market case study in Miami-Dade, Florida. *Population Research and Policy Review*, 37(6), 871–895.
- McPhearson, T.; Karki, M.; Herzog, C.; Santiago Fink, H.; Abbadie, L.; Kremer, P.; Clark, C.M.; Palmer, M.I., and Perini, K., 2018. Urban ecosystems and biodiversity. *In:* Rosenzweig, C.; Solecki, W.; Romero-Lankao, P.; Mehrotra, S.; Dhakal, S., and Ali Ibrahim, S. (eds.), *Climate Change and Cities: Second Assessment Report of the Urban Climate Change Research Network*. New York: Cambridge University Press, pp. 257–318.
- Mendelsohn, R.; Emanuel, K.; Chonabayashi, S., and Bakkensen, L., 2012. The impact of climate change on global tropical cyclone damage. Nature Climate Change, 2, 205–209. doi:10.1038/NCLIMATE1357
- Miller, J.K. and Livermont, E., 2008. A predictive index for wave and storm surge induced erosion. *Proceedings of the 31st International Conference on Coastal Engineering* (Hamburg, Germany), pp. 4143–4153.
- Mulia, I.E.; Ueda, N.; Miyoshi, T.; Iwamoto, T., and Heidarzadeh, M., 2023. A novel deep learning approach for typhoon-induced storm surge modeling through efficient emulation of wind and pressure fields. Scientific Reports, 13, 7918. doi:10.1038/s41598-023-35093-9
- Narayan, S.; Beck, M.W.; Reguero, B.G.; Losada, I.J.; van Wesenbeeck, B.; Pontee, N.; Sanchirico, J.N.; Ingram, J.C.; Lange, G.-M., and Burks-Copes, K.A., 2016. The effectiveness, costs and coastal protection benefits of natural and nature-based defences. *PLoS ONE*, 11(5), e0154735.
- Palm, R. and Bolsen, T., 2023. Perspectives of southwest Florida homeowners and real estate agents before Hurricane Ian. *The Professional Geographer*, 75(6), 916–931. doi:10.1080/00330124.2023.2194372
- Peduzzi, P.; Chatenoux, B.; Dao, H.; De Bono, A.; Herold, C.; Kossin, J.; Mouton, F., and Nordbeck, O., 2012. Global trends in tropical cyclone risk. *Nature Climate Change*, 2, 289–294. doi:10.1038/NCLIMATE1410

- PIANC (The World Association for Waterborne Transport Infrastructure), 2011. PIANC Position Paper: Working with Nature. www.pianc.org/downloads/envicom/WwN%20Final%20position%20paper%20January% 202011.pdf
- Pielke R.A., Jr.; Gratz, J.; Landsea, C.W.; Collins, D.; Saunders, M.A., and Musulin, R., 2008. Normalized hurricane damage in the United States: 1900–2005. Natural Hazards Review, 9(1), 29–42.
- Reguero, B.G.; Beck, M.W.; Bresch, D.N.; Calil, J., and Meliane, I., 2018. Comparing the cost effectiveness of nature-based and coastal adaptation: A case study from the Gulf Coast of the United States. *PLoS ONE*, 13(4), e0192132.
- Resio, D.T. and Westerink, J.J., 2008. Modeling the physics of storm surges. *Physics Today*, 61(9), 33–38.
- Roberts, T.M.; Wang, P., and Puleo, J.A., 2013. Storm-driven cyclic beach morphodynamics of a mixed sand and gravel beach along the Mid-Atlantic coast, USA. *Marine Geology*, 346, 403–421.
- Sallenger, A.H., 2000. Storm impact scale for barrier islands. *Journal of Coastal Research*, 16(3), 890–895.
- Simpson, N.P.; Mach, K.J.; Constable, A.; Hess, J.; Hogarth, R.; Howden, M.; Lawrence, J.; Lempert, R.J.; Muccione, V.; Mackey, B.; New, M.G.; O'Neill, B.; Otto, F.; Pörtner, H.-O.; Reisinger, A.; Roberts, D.; Schmidt, D.N.; Seneviratne, S.; Strongin, S.; van Aalst, M.; Totin, E., and Trisos, C.H., 2021. A framework for complex climate change risk assessment. *One Earth*, 4(4), 489–501. doi:10. 1016/j.oneear.2021.03.005
- Sweet, W.V.; Hamlington, B.D.; Kopp, R.E.; Weaver, C.P.; Barnard, P.L.; Bekaert, D.; Brooks, W.; Craghan, M.; Dusek, G.; Frederikse, T.; Garner, G.; Genz, A.S.; Krasting, J.P.; Larour, E.; Marcy, D.; Marra, J.J.; Obeysekera, J.; Osler, M.; Pendleton, M.; Roman, D.; Schmied, L.; Veatch, W.; White, K.D., and Zuzak, C., 2022. Global and Regional Sea Level Rise Scenarios for the United States: Updated Mean Projections and Extreme Water Level Probabilities along U.S. Coastlines. Silver Spring, Maryland: National Oceanic and Atmospheric Administration, National Ocean Service, NOAA Technical Report NOS 01, 111p. https://oceanservice.noaa.gov/hazards/sealevelrise/noaanostechrpt01-global-regional-SLR-scenarios-US.pdf

- Thompson, V.D.; Marquardt, W.H.; Savarese, M.; Walker, K.J.; Newsom, L.A.; Lulewicz, I.; Lawres, N.R.; Roberts-Thompson, A.D.; Bacon, A.R., and Walser, C.A., 2020. Ancient engineering of fish capture and storage in southwest Florida. Proceedings of the National Academy of Sciences of the United States of America, 117(15), 8374–8381. https://doi.org/10.1073/pnas.1921708117.
- Wamsley, T.V.; Cialone, M.A.; Smith, J.M.; Atkinson, J.H., and Rosati, J.D., 2010. The potential of wetlands in reducing storm surge. Ocean Engineering, 37(1), 59–68.
- Wamsley, T.V.; Cialone, M.A.; Smith, J.M., and Ebersole, B.A., 2009a.
 Influence of landscape restoration and degradation on storm surge and waves in southern Louisiana. *Journal of Natural Hazards*, 51(1), 207–224.
- Wamsley, T.V.; Cialone, M.A.; Westerink, J., and Smith, J.M., 2009b.
 Numerical Modeling System to Simulate Influence of Marsh Restoration and Degradation on Storm Surge and Waves. Vicksburg, Mississippi: U.S. Army Engineer and Research Development Center, ERDC/CHL CHETN-I-77.
- Wang, P.; Kirby, J.H.; Haber, J.D.; Horwitz, M.H.; Knorr, P.O., and Krock, J.R., 2006. Morphological and sedimentological impacts of Hurricane Ivan and immediate poststorm beach recovery along the northwestern Florida Barrier-Island Coasts. *Journal of Coastal Research*, 22(6), 1382–1402.
- Wang, P.; Adam, J.D.; Cheng, J., and Vallée, M., 2020. Morphological and sedimentological impacts of Hurricane Michael along the northwest Florida coast. *Journal of Coastal Research*, 36(5), 932–950.
- Wang, P. and Beck, T.M., 2022. Beach-Inlet Interaction and Sediment Management. Cambridge: Cambridge University Press, 364p.
- Wang, P. and Horwitz, M.H., 2007. Erosional and depositional characteristics of regional overwash deposits caused by multiple hurricanes. Sedimentology, 54(3), 545–564.
- Woodruff, J.D.; Irish, J.L., and Camargo, S.J., 2013. Coastal flooding by tropical cyclones and sea-level rise. *Nature*, 504, 44–52. doi:10.1038/ nature12855